

# 1 Dosage of duplicated and antifunctionalized homeobox proteins 2 influences spikelet development in barley

3  
4 Venkatasubbu Thirulogachandar<sup>1,5,\*</sup>, Geetha Govind<sup>1,a</sup>, Götz Hensel<sup>1,b</sup>, Sandip M.  
5 Kale<sup>1</sup>, Markus Kuhlmann<sup>1,5</sup>, Lennart Eschen-Lippold<sup>2,c</sup>, Twan Rutten<sup>1</sup>, Ravi Koppolu<sup>1</sup>,  
6 Jeyaraman Rajaraman<sup>1</sup>, Sudhakar Reddy Palakolanu<sup>1,f</sup>, Christiane Seiler<sup>1</sup>, Shun  
7 Sakuma<sup>3,d</sup>, Murukarthick Jayakodi<sup>1</sup>, Justin Lee<sup>2</sup>, Jochen Kumlehn<sup>1</sup>, Takao  
8 Komatsuda<sup>3,g</sup>, Thorsten Schnurbusch<sup>1,4,\*</sup>, and Nese Sreenivasulu<sup>1,5,e,\*</sup>

9  
10 <sup>1</sup> Leibniz Institute of Plant Genetics and Crop Plant Research (IPK), Corrensstr. 3,  
11 OT Gatersleben, D-06466 Stadt Seeland, Germany

12  
13 <sup>2</sup> Leibniz Institute of Plant Biochemistry (IPB), Weinberg 3, D-06120 Halle, Germany

14  
15 <sup>3</sup> National Institute of Agrobiological Sciences (NIAS), Plant Genome Research Unit,  
16 Tsukuba 3058602, Japan

17  
18 <sup>4</sup> Institute of Agricultural and Nutritional Sciences, Faculty of Natural Sciences III,  
19 Martin Luther University Halle-Wittenberg, 06120 Halle, Germany

20  
21 <sup>5</sup> Research Group Abiotic Stress Genomics, Interdisciplinary Center for Crop Plant  
22 Research (IZN), Hoher Weg 8, 06120 Halle (Saale), Germany

## 24 Present address

25 <sup>a</sup>Department of Crop Physiology, College of Agriculture, Hassan, 573225, Karnataka,  
26 India

27  
28 <sup>b</sup>Institute of Plant Biochemistry, Heinrich Heine University, 40225 Düsseldorf,  
29 Germany

30  
31 <sup>d</sup>Faculty of Agriculture, Tottori University, Tottori 680-8550, Japan

32  
33 <sup>c</sup>Department of Crop Physiology, Institute of Agricultural and Nutritional Sciences,  
34 Martin Luther University, 06120 Halle-Wittenberg, Germany

35  
36 <sup>e</sup> International Rice Research Institute (IRRI), Grain Quality and Nutrition Center,  
37 DAPO Box 7777, Metro Manila, Philippines

38  
39 <sup>f</sup>Cell, Molecular Biology and Trait Engineering Cluster, International Crops Research  
40 Institute for the Semi-Arid Tropics (ICRISAT), Hyderabad, 502 324, Telangana, India

41  
42 <sup>g</sup>Crop Research Institute, Shandong Academy of Agricultural Sciences (SAAS),  
43 Jinan, Shandong 250100, China

## 44 45 \*Corresponding authors

46 Sreenivasulu, N. ([n.sreenivasulu@irri.org](mailto:n.sreenivasulu@irri.org))

47 Schnurbusch, T. ([schnurbusch@ipk-gatersleben.de](mailto:schnurbusch@ipk-gatersleben.de))

48 Thirulogachandar, V. ([venkatasubbu@ipk-gatersleben.de](mailto:venkatasubbu@ipk-gatersleben.de))

51  Lead contact

52 Thirulogachandar, V ([venkatasubbu@ipk-gatersleben.de](mailto:venkatasubbu@ipk-gatersleben.de))

53  
54 Short title: HD-ZIP I TFs influence spikelet development

55  
56 The authors responsible for distribution of materials integral to the findings presented  
57 in this article in accordance with the policy described in the Instructions for Authors  
58 (<https://academic.oup.com/plcell/pages/General-Instructions>) are: Sreenivasulu, N.  
59 ([n.sreenivasulu@irri.org](mailto:n.sreenivasulu@irri.org)); Schnurbusch, T. ([schnurbusch@ipk-gatersleben.de](mailto:schnurbusch@ipk-gatersleben.de));  
60 Thirulogachandar, V. ([venkatasubbu@ipk-gatersleben.de](mailto:venkatasubbu@ipk-gatersleben.de))

61  
62 ORCID

63 Venkatasubbu Thirulogachandar - 0000-0002-7814-5475

64 Geetha Govind - 0000-0003-0450-0814

65 Sandip M. Kale - 0000-0003-0665-509

66 Markus Kuhlmann - 0000-0003-3104-0825

67 Lennart Eschen-Lippold - 0000-0001-8907-6922

68 Götz Hensel - 0000-0002-5539-3097

69 Twan Rutten - 0000-0001-5891-6503

70 Ravi Koppolu - 0000-0001-8566-9501

71 Jeyaraman Rajaraman - 0000-0003-0946-0508

72 Sudhakar Reddy Palakolanu – 0000-0002-5341-187X

73 Christiane Seiler - 0000-0001-7181-9855

74 Shun Sakuma - 0000-0003-1622-5346

75 Murukarthick Jayakodi - 0000-0003-2951-0541

76 Justin Lee - 0000-0001-8269-7494

77 Dierk Scheel - 0000-0002-2105-6711

78 Jochen Kumlehn - 0000-0001-7080-7983

79 Takao Komatsuda -

80 Thorsten Schnurbusch - 0000-0002-5267-0677

81 Nese Sreenivasulu - 0000-0002-3998-038X

82

83

84

85

86

87

88

89

90

91

92

93

94

95

96 **Abstract**

97 Illuminating the mechanisms of inflorescence architecture of grain crops that feed our  
98 world may strengthen the goal towards sustainable agriculture. Lateral spikelet  
99 development of barley (*Hordeum vulgare* L.) is such an example of a floral architectural  
100 trait regulated by VRS1 (Vulgare Row-type Spike 1 or Six-rowed Spike 1, syn.  
101 HvHOX1). Its lateral spikelet-specific expression and the quantitative nature of  
102 suppressing spikelet development were previously shown in barley. However, the  
103 mechanistic function of this gene and its paralog HvHOX2 on spikelet development is  
104 still fragmentary. Here, we show that these duplicated transcription factors (TFs) have  
105 contrasting nucleotide diversity in various barley genotypes and several *Hordeum*  
106 species. Despite this difference, both proteins retain their basic properties of the  
107 homeodomain leucine zipper class I family of TFs. During spikelet development, these  
108 genes exhibit similar spatiotemporal expression patterns yet with anticyclic expression  
109 levels. A gene co-expression network analysis suggested that both have an ancestral  
110 relationship but their functions appear antagonistic to each other, i.e., HvHOX1  
111 suppresses whereas HvHOX2 rather promotes spikelet development. Our transgenic  
112 promoter-swap analysis showed that HvHOX2 can restore suppressed lateral spikelets  
113 when expression levels are increased; however, at its low endogenous expression  
114 level, HvHOX2 appears dispensable for spikelet development. Collectively, this study  
115 proposes that the dosage of the two antagonistic TFs, HvHOX1 and HvHOX2,  
116 influence spikelet development in barley.

117

118 **Keywords**

119 Inflorescence architecture, lateral spikelet, HD-ZIP class I transcription factors,  
120 duplication, antagonistic transcription factors, antifunctionalization, homeobox  
121 transcription factors, RNA-guided Cas9 endonuclease, site-directed mutagenesis,  
122 nucleotide diversity, dosage of expression.

123

124

125

126

127

128 **Introduction:**

129 Cereals such as maize (*Zea mays* L.), rice (*Oryza sativa* L.), wheat (*Triticum* spp.), and  
130 barley (*Hordeum vulgare* L.) are major grass species that feed most of the population  
131 on earth. Understanding the genetic regulation of inflorescence (flower-bearing  
132 structure) architecture in these cereal crops may shed light on the basic developmental  
133 patterning of floral meristems and reveal potential pathways to improve their yield.  
134 Barley, along with other major cereal crops (wheat, rye, and triticale) belonging to the  
135 *Triticeae* tribe, possesses a branchless inflorescence known as 'spike' (Ullrich, 2011;  
136 Koppolu and Schnurbusch, 2019). In general, a barley spike forms three spikelets on  
137 its rachis (inflorescence axis) nodes – one central and two lateral spikelets in an  
138 alternating, opposite arrangement (distichous) (Bonnett, 1935; Koppolu and  
139 Schnurbusch, 2019; Zwirek et al., 2019). The spikelet, a small/condensed spike, is  
140 considered the basic unit of the grass inflorescence (Clifford et al., 1987; Kellogg et al.,  
141 2013). A barley spikelet forms a single floret that is subtended by a pair of glumes.  
142 Typically, a barley floret consists of one lemma, one palea, two lodicules, three  
143 stamens, and a monocarpellary pistil (i.e., single carpel) (Waddington et al., 1983;  
144 Forster et al., 2007). Based on the fertility of the lateral spikelets/florets, barley is  
145 classified into two- and six-rowed spike types. In two-rowed types, the lateral spikelets  
146 are smaller (compared to the central spikelets), awnless (extension of the lemma is  
147 absent), and sterile, while the central spikelets are bigger, awned, and fertile. In six-  
148 rowed types, both the lateral and central spikelets are awned and fertile.

149 The major gene responsible for the lateral spikelet fertility was found to be a  
150 homeodomain leucine zipper class I (HD-ZIP I) transcription factor, known as *VRS1*  
151 (*Vulgare Row-type Spike1* or *Six-rowed Spike 1*, syn *HvHOX1*) (Komatsuda et al.,  
152 2007). Transcripts and proteins of *HvHOX1* had previously been found in barley spikes,  
153 predominantly in the lateral florets and most strongly in the carpels, corroborating a  
154 role of *HvHOX1* as negative regulator of lateral floret development and fertility  
155 (Komatsuda et al., 2007; Sakuma et al., 2010; Sakuma et al., 2013). Recently, a very  
156 similar function has also been identified for its orthologous wheat gene during apical  
157 floret abortion(Sakuma et al., 2019). In recent years, *HvHOX1* was shown to be also  
158 expressed in other organs, such as leaves, where in analogy to its effects on lateral  
159 spikelet development, it negatively affects the size of leaf primordia and results in  
160 narrower leaves in two-rowed barleys (Thirulogachandar et al., 2017). Further  
161 supporting its suppressive function, one specific allele of *HvHOX1* is responsible for

162 the extremely reduced lateral spikelet size in *deficiens* barley (Sakuma et al., 2017).  
163 Interestingly, *HvHOX2*, the paralog of *HvHOX1*, was also identified in barley. Although  
164 *HvHOX2* is expressed in a wide variety of organs including leaves, coleoptile, root, and  
165 spike; tissue-wise, it is mainly found in vascular regions particularly those at the base  
166 of lateral spikelets (pedicel) and rachis, thus suggesting a role in the promotion of  
167 development (Sakuma et al., 2010; Sakuma et al., 2011; Sakuma et al., 2013). In  
168 addition to *HvHOX1*, four other genes, *VRS2*, *VRS3*, *VRS4*, and *VRS5* or *INT-C*  
169 (*intermedium-spike c*), were reported to be involved in the suppression of lateral  
170 spikelet fertility (Ramsay et al., 2011; Koppolu et al., 2013; Bull et al., 2017; van Esse  
171 et al., 2017; Youssef et al., 2017). Notably, *VRS4*, the ortholog of maize *RAMOSA2*  
172 (RA2) appeared to be functionally upstream of *HvHOX1* but not of *HvHOX2* (Koppolu  
173 et al., 2013; Sakuma et al., 2013). Later, *VRS3* was also identified as an upstream  
174 regulator of *HvHOX1*, and in certain stages also of *HvHOX2* (Bull et al., 2017; van  
175 Esse et al., 2017).

176 Despite the detailed studies on *HvHOX1*'s expression pattern and mutants, the  
177 mechanistic role of *HvHOX1* on barley spikelet development is still unclear. The same  
178 holds true for *HvHOX2* while its suggested role in barley development has yet to be  
179 validated (Sakuma et al., 2010; Sakuma et al., 2013). In this study, we show that  
180 *HvHOX1* and *HvHOX2* proteins are functional HD-ZIP class I transcription factors. Our  
181 transcript expression studies suggest that both have similar spatiotemporal expression  
182 patterns; however, with a contrasting dosage of transcripts in central and lateral  
183 spikelets during spikelet development. Based on our combined results, we conclude  
184 that both genes are ancestrally related but act antagonistically to each other, i.e.,  
185 *HvHOX1* suppresses whereas *HvHOX2* rather promotes spikelet development. Our  
186 transgenic promoter-swap analysis shows that *HvHOX2* can restore suppressed  
187 lateral spikelets when transcript levels are increased, most likely, by modulating the  
188 adverse effects caused by *HvHOX1*. At low endogenous transcript levels, however,  
189 *HvHOX2* appears dispensable for spikelet development. Collectively, our findings  
190 recommend that *HvHOX1* and *HvHOX2* act antagonistic to each other, and that the  
191 dosage of their transcripts influences barley spikelet development.

192

193

194 **Results:**

195 ***HvHOX2* nucleotide diversity is highly conserved compared to its paralog**

196 ***HvHOX1***

197 The eight different natural alleles for *HvHOX1* known so far are grouped into two-rowed  
198 (*Vrs1.b2*, *Vrs1.b3*, *Vrs1.b5*, & *Vrs1.t1*) and six-rowed alleles (*vrs1.a1*, *vrs1.a2*, *vrs1.a3*,  
199 & *vrs1.a4*) (Komatsuda et al., 2007; Sakuma et al., 2017; Casas et al., 2018). In  
200 contrast, the nucleotide diversity of *HvHOX2* is largely unknown. To fill this gap, we  
201 sequenced the *HvHOX2* promoter (one kb) and gene (including 5' and 3' untranslated  
202 region) in 83 diverse spring barleys (44 two-rowed and 39 six-rowed). Surprisingly, we  
203 found only four single nucleotide polymorphisms (SNPs), restricted to the promoter  
204 (two SNPs), 5'UTR (one SNP), and intron-2 (one SNP). At the same time, the coding  
205 sequence (CDS) was identical and highly conserved in all these accessions  
206 (Supplementary Table 1). We further expanded our nucleotide diversity study by  
207 sequencing the *HvHOX1* and *HvHOX2* in 24 *Hordeum* spp. (Supplementary Table 2),  
208 which showed that the non-synonymous (*Ka*) and synonymous (*Ks*) substitution values  
209 of *HvHOX1* (*Ka* = 0.028, *Ks* = 0.049) and *HvHOX2* (*Ka* = 0.008, *Ks* = 0.051). The  
210 higher *Ka* value of *HvHOX1* than that of *HvHOX2* indicates that the evolutionary speed  
211 of *HvHOX1* is much faster than that of *HvHOX2*, otherwise, *HvHOX2* has been well  
212 conserved among the *Hordeum* species (Supplementary Table 3). A subsequent  
213 comparison of the nucleotide diversity ( $\pi$ ) of these two genes (*HvHOX2*, Chr.2H:  
214 139932435-139953386; *HvHOX1*, Chr.2H: 581356498-581377358) in 200  
215 domesticated barleys (Jayakodi et al., 2020) confirmed the lower nucleotide diversity  
216 ( $\pi$ ) of *HvHOX2* compared to *HvHOX1* (Supplementary Fig. 1A). The study also  
217 revealed two major haplotypes for the *HvHOX2* genic region, whereas *HvHOX1*  
218 possesses multiple haplotypes that span the whole region analyzed (Supplementary  
219 Fig. 1B). This difference in diversity might be due to their physical location, wherein  
220 *HvHOX1* is located in the distal end of the high recombining region of chromosome  
221 2H, while *HvHOX2* is closer to the centromeric region on 2H. Concertedly, all the above  
222 results indicate that *HvHOX2* is highly conserved compared to its paralog *HvHOX1*.  
223

224 ***HvHOX1* and *HvHOX2* are functional HD-ZIP class I transcription factors**

225 In general, members of the HD-ZIP family (class I to IV) of transcription factors possess  
226 a homeodomain (HD) followed by a leucine zipper motif (LZ). The LZ motif enables the  
227 dimerization of HD-ZIP proteins, which bind to their specific DNA target (cis-element)

228 via the HD motif (Ariel et al., 2007). The HD-ZIP class I proteins - HvHOX1 and  
229 HvHOX2 show a very high sequence identity between their HD (89.3 %) and LZ (90 %)  
230 motifs. However, they have several amino acid changes across their protein with yet  
231 unknown consequences (Supplementary Fig. 2). In particular, HvHOX1 lacks a  
232 putative AHA-like motif in its C-terminus, which was predicted to be an interaction motif  
233 with the basal transcriptional machinery (Arce et al., 2011; Capella et al., 2014)  
234 (Supplementary Fig. 2). All these similarities and discrepancies paved the way to  
235 compare the functionality of these two proteins.

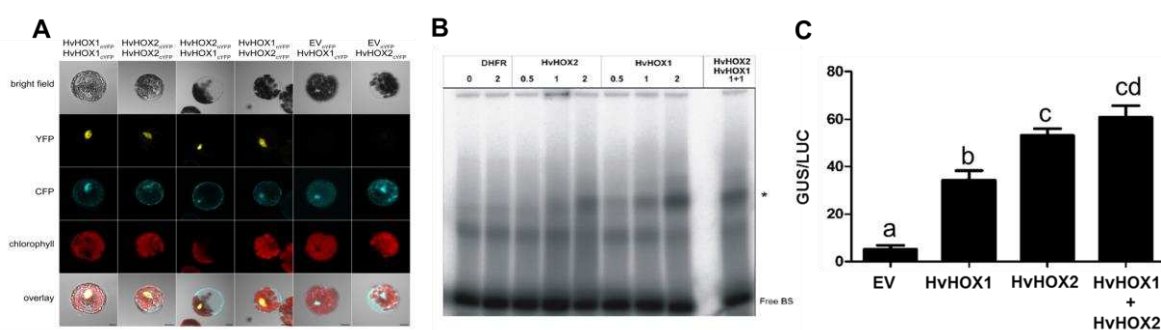


**Figure 1: HvHOX1 and HvHOX2 are functional HD-ZIP class I transcription factors.**

Bimolecular fluorescence complementation assay (BiFC) for HvHOX1 and HvHOX2 proteins is shown (A). The bright field panel displays the protoplast in which the results were captured; YFP (Yellow Fluorescent Protein) panel reveals the dimer formation with the yellow color fluorescence, and CFP (Cyan Fluorescent Protein) panel discloses the location of the nucleus (blue, dark spot), and the autofluorescence of chlorophyll (red signal) is seen in the chlorophyll panel. The last overlay panel exhibits the merged signals from the above three panels. nYFP-YFP fused to N-terminal; cYFP-YFP fused to C-terminal end. Scale bar 10  $\mu$ m. B) The DNA binding specificity of HvHOX1 and HvHOX2 proteins on HD-Zip I cis-element assessed by Electro Mobility Shift Assay (EMSA) is shown. Three different concentrations (0.5  $\mu$ L, 1  $\mu$ L, and 2  $\mu$ L) of protein were used along with the DNA fragment containing the HD-Zip I cis-element (Binding sequence, BS). The shift of protein-DNA complex (\*) denotes the specific DNA binding of these proteins. Also, a combination of HvHOX1 and HvHOX2 proteins (1  $\mu$ L from each) also shows the protein-DNA complex. Dihydrofolate reductase (DHFR) was used as a negative control. BS- binding sequence (HD-Zip I cis element); Free BS- unbound BS; different numbers show the *in vitro* translated protein volume in  $\mu$ L. C) The transactivation property of HvHOX1 and HvHOX2 proteins is shown. Bar plot indicates the detected GUS activity relative to luciferase (LUC). Data shown are mean  $\pm$  SE (n=3); different letters (a, b, c, and d) indicate that the mean values are significantly different at the 1% probability level, by One-way ANOVA with Newman-Keuls Multiple Comparison Test; EV- empty vector, pGAL4-4xUAS::GUS; HvHOX1- construct of GAL4-DNA binding domain fused to N-terminus of HvHOX1; HvHOX2- GAL4-DNA binding domain fused to N-terminus of HvHOX2; LUC- luciferase used for normalization; GUS-  $\beta$ -glucuronidase

237  
238 We assessed the dimerization properties of HvHOX1 and HvHOX2 with the  
239 bimolecular fluorescence complementation assay. *HvHOX1* and *HvHOX2* were cloned  
240 into split-Yellow Fluorescence Protein (YFP) vectors creating N-terminal c-myc-nYFP  
241 and HA-cYFP fusions. The resulting plasmids were co-transformed with a Cyan  
242 Fluorescent Protein (CFP) construct into *Arabidopsis* mesophyll protoplasts. The CFP  
243 served as a transformation control, accumulating in the nucleus and cytoplasm. The  
244 detection of yellow fluorescence in all four combinations indicated that the HvHOX1  
245 and HvHOX2 proteins are able to form homo- or heterodimers (Fig. 1A). The  
246 superimposed YFP channel (dimerization) on the CFP channel (strong nuclear signal)

247 indicated that homo- or heterodimers of both proteins are localized in the nucleus (Fig.  
248 1A), which is in agreement with the nuclear localization signals predicted for both  
249 proteins (Sakuma et al., 2013). This localization also implied that these dimers might  
250 bind to their *cis*-elements to transactivate their downstream genes (Fig. 1A). A western  
251 blot analysis using antibodies directed against HA and c-myc epitopes confirmed that  
252 the proteins were expressed in full-length and at similar levels (Supplementary Fig. 3).  
253 Following, we verified the DNA binding properties of HvHOX1, and HvHOX2 with an  
254 electromobility shift assay (EMSA) using the *in vitro* translated proteins and  
255 experimentally verified *HD-Zip* I *cis*-element from Sessa et al. (1993)(Sessa et al.,  
256 1993). A clear shift of protein-DNA bands (marked with \*) was detected for both  
257 proteins, especially in higher concentrations of proteins, which indicated binding to the  
258 *HD-Zip* I *cis*-element (Fig. 1B). The result further suggested that HvHOX1 might have  
259 a more potent DNA binding property than HvHOX2 (Fig. 1B). We then conducted a *cis*-  
260 element competition assay to evaluate the binding specificity of the proteins to the *HD-*  
261 *Zip* I *cis*-element. Intriguingly, we observed binding of HvHOX1 to *HvHOX2* promoter  
262 and mild interactions of HvHOX2 with the *HvHOX1* and *HvHOX2* promoters  
263 (Supplementary Fig. 4). This suggests that *in vivo*, HvHOX1 potentially influences  
264 *HvHOX2* expression, similarly, HvHOX2 modulates *HvHOX1* expression.

265 After the dimerization and DNA binding studies, we investigated the transactivation  
266 property of these proteins *in vivo* using an *Arabidopsis* mesophyll protoplast system.  
267 We found that both proteins have transactivating properties, which were quantified and  
268 compared with the empty vector. Interestingly, the transactivation property of HvHOX2  
269 was significantly higher compared to that of HvHOX1 (Fig. 1C). Collectively, all of the  
270 above results exemplified that both HvHOX1 and HvHOX2 possess DNA binding  
271 activity, can form homo- and heterodimers, and have transactivation potential, which  
272 corroborated that both proteins are functional HD-ZIP class I transcription factors.

273

## 274 **Two-rowed spikes have delayed lateral spikelet initiation and reduced growth**

275 The size and fertility of lateral spikelets determine the row-type and intermedium-spike  
276 types in barley (Komatsuda et al., 2007; Ramsay et al., 2011; Youssef et al., 2017;  
277 Zwirek et al., 2019). To comprehend the differences of lateral and central spikelets in  
278 two-rowed barley, we tracked these spikelets from their early initiation until pollination  
279 in the two-rowed cv. Bowman. Barley spike development starts from the double ridge  
280 (DR) stage, in which spikelet ridges are subtended by leaf ridges (Fig. 2A). In the next

281 stage, known as 'triple mound' (TM), the spikelet ridge differentiates into one central

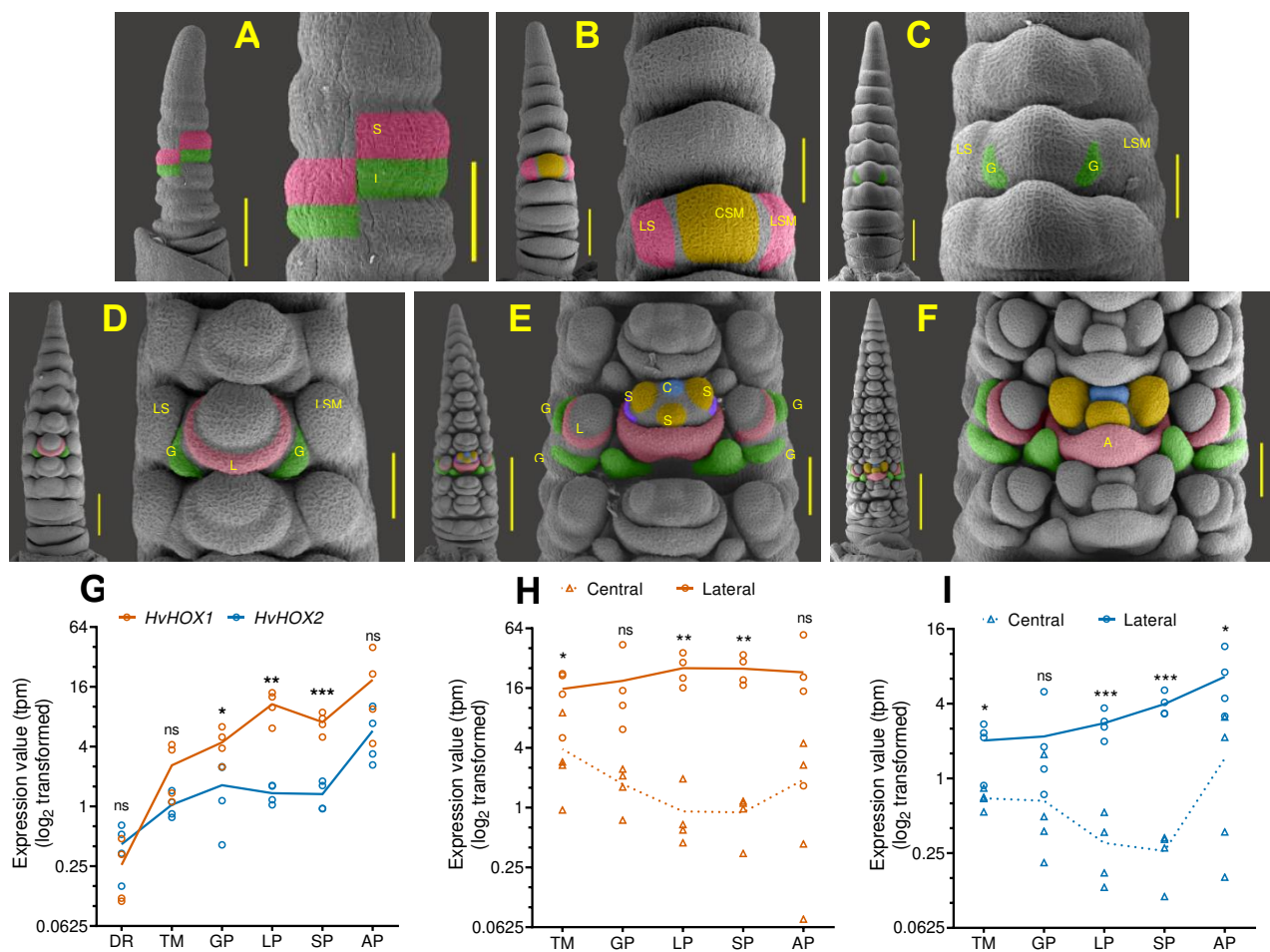


**Figure 2: Two-rowed spikes have delayed lateral spikelet initiation and reduced growth.**

Early spike developmental stages of a two-rowed cultivar Bowman are shown from A to F. Double ridge (DR) is shown in A, in which the spikelet ridge (SR) is subtended by a leaf ridge (LR). The SR differentiates into one central and two lateral spikelet meristems (CSM & LSM) at triple mound stage (TM), which is displayed in B. Panel C discloses the appearance of two glume primordia (GP) from the CSM, while the two LSMs do not show any sign of differentiation. Subsequently, the CSM further differentiates and forms a lemma primordium (LP), which is shown in D. Two GP and a sign of LP initiation from the LSM can be seen in the panel E; the CSM initiated three stamen primordia along with a sign of carpel primordia development at this stage. At awn primordium stage (AP), F, the CSM completed the formation of all floral organ primordia (including the carpel), and the AP initiates from the medial point of the LP. However, the laterals are found only with two GP and a LP. Panels G, H, and I depicts the expression pattern of *HvHOX1* and *HvHOX2* genes in the whole spikes of DR to AP stages, *HvHOX1* and *HvHOX2* in the central and lateral spikelets of TM to AP stages, respectively. *HvHOX1* expresses higher than *HvHOX2* in the whole spikes of GP, LP, and SP stages (G). Both the genes are expressed in the dissected central and lateral spikelets from TM to AP stages. Mean values of G-I are compared with the multiple Student's *t*-test; \*, \*\*, \*\*\*, mean values are significantly different at 5, 1, and 0.1% probability levels; ns-not significantly different. Scale bar in panel A - whole spike 500  $\mu$ m, magnified three nodes 100  $\mu$ m; B & C-500  $\mu$ m & 200  $\mu$ m; D- 500  $\mu$ m & 100  $\mu$ m; E & F-200  $\mu$ m & 100  $\mu$ m. W-Waddington scale.

282 and two lateral spikelet meristems (CSM & LSM), in which the CSM develops as a  
 283 bigger structure compared to the two LSMs (Fig. 2B). This marks the first difference  
 284 between the central and lateral spikelets. Following the TM stage, the CSM continues  
 285 to differentiate into various spikelet/floret organ primordia (glume, lemma, palea,  
 286 stamen, pistil, and awn) (Fig. 2C-F). From the glume primordium stage, however, the

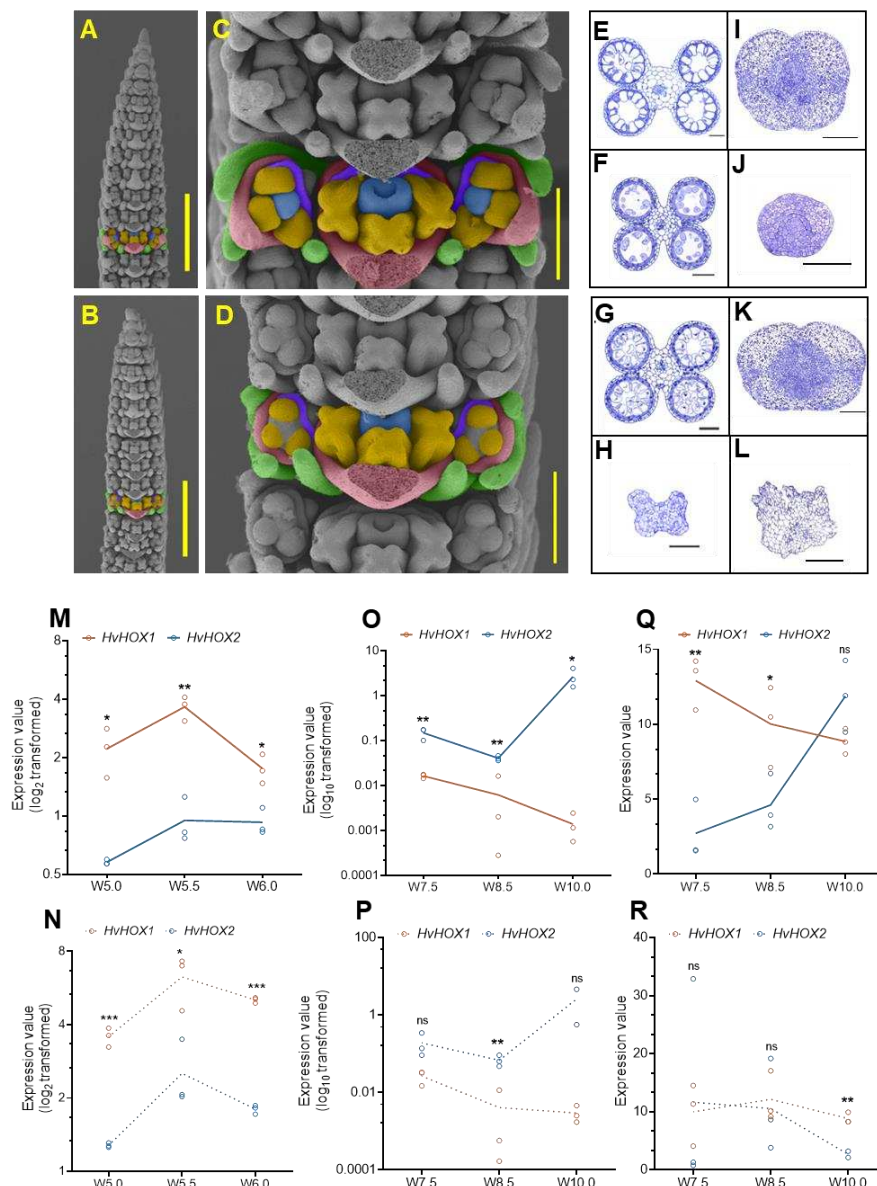
287 LSM exhibits a delayed differentiation indicating the suppression of LSM (Fig. 2C). At  
288 the awn primordium stage (AP), the central spikelets have completed the differentiation  
289 of all spikelet/floret organs, while the laterals only achieved the differentiation of glume  
290 and lemma (Fig. 2F). We also compared the development of lateral spikelets between  
291 the two-rowed cv. Bowman and its near-isogenic six-rowed line BW-NIL(*vrs1.a*) (Druka  
292 et al., 2011). Close to the white anther stage (Kirby and Appleyard, 1984), the  
293 difference between the laterals of two- and six-rowed spikes became apparent (Fig.  
294 3A-D). The six-rowed laterals possessed primordia for all spikelet/floret organs,  
295 whereas in two-rowed, laterals had retarded awn and pistil primordia (Fig. 3C & D). We  
296 also verified the divergence of lateral spikelet development in another pair of two- (cv.  
297 Bonus) and six-rowed (*hex-v.3, vrs1* deletion mutant) barleys (Supplementary Fig. 5).  
298 To fathom the sterility of lateral spikelets, we compared the histology of pistil and anther  
299 growth in Bowman and its *vrs1.a* mutant [BW-NIL(*vrs1.a*)] from Waddington stage 4.5  
300 (W4.5, awn primordium stage) to W10.0 (pollination) (Supplementary Fig. 6&7). The  
301 delayed differentiation of lateral spikelets observed during the spikelet initiation stages  
302 (TM to AP) continued in the growth stages of the reproductive organs (Fig. 3E-L).  
303 Anthers of two-rowed lateral spikelets showed an impeded differentiation compared to  
304 the anthers of other spikelets (Supplementary Fig. 6, A3-J3). However, the central  
305 spikelet anthers of two- (Supplementary Fig. 6, A1-J1) and six-rowed (Supplementary  
306 Fig. 6, A2-J2) exhibited an advanced progression rate across the stages. Notably, the  
307 six-rowed lateral anther (Supplementary Fig. 6, A4-J4) followed a differentiation rate  
308 between the two- and six-rowed centrals as well as the two-rowed laterals, indicating  
309 that there are additional suppressors of lateral spikelet development besides HvHOX1.  
310 Moreover, anthers of the two-rowed lateral spikelets stopped differentiation at W7.5  
311 (Supplementary Fig. 6, E3), followed by tissue disintegration in the subsequent stages  
312 (Supplementary Fig. 6, E3 to J3). In contrast, all other anthers continued their growth  
313 towards pollination (Supplementary Fig. 6). A similar delay of differentiation and  
314 disintegration of tissues was also observed in the pistil of two-rowed laterals at W7.5  
315 (Supplementary Fig. 7, C5). Concertedly, these results substantiate that two-rowed  
316 spikes have delayed lateral spikelet initiation and suppressed growth compared to their  
317 central and all the spikelets of six-rowed spikes. Eventually, the reproductive organs of  
318 the lateral spikelets in two-rowed cv. Bowman abort during the later growth phase.  
319

320 ***HvHOX1* and *HvHOX2* have a contrasting dosage of expression during spikelet  
321 initiation and growth**

322 We have taken the  $\log_2$  transformed expression values of *HvHOX1* and *HvHOX2* from  
323 the Bowman RNA-seq spike atlas data (Thiel et al., 2021) and reanalyzed them to find  
324 their expression pattern across the spikelet initiation stages (Fig. 2G-I). In the tissue-  
325 unspecific (central and lateral combined or whole spike) transcript analysis, both genes  
326 showed a linear increase in expression along with the spikelet initiation stages (Fig.  
327 2G). With the exception of the DR stage, *HvHOX1* generally displayed higher transcript  
328 levels than *HvHOX2* (TM to AP). This was particularly evident in glume primordium  
329 (GP), lemma primordium (LP), and stamen primordium (SP) stages (Fig. 2G). We then  
330 compared the tissue-specific expression patterns of these genes in central and lateral  
331 spikelets. Notably, both genes had higher levels of mRNA in the laterals than centrals  
332 at TM, LP, and stamen primordium (SP) stages (Fig. 2H & I). Then, we compared the  
333 expression level of these genes within the same tissues (central and lateral spikelets),  
334 in which *HvHOX1* showed significantly higher expression than *HvHOX2* in several  
335 stages (TM, LP, & SP) of lateral and at the SP stage of central spikelets  
336 (Supplementary fig. 8A & B). The high expression of *HvHOX1* in the laterals correlates  
337 with the delayed differentiation and suppression of the lateral spikelets (compared to  
338 the centrals) from the TM to AP stages in Bowman (Supplementary Fig. 8B). This  
339 reinforced the role of *HvHOX1* as a negative regulator of lateral spikelet development  
340 in barley (Komatsuda et al., 2007; Sakuma et al., 2010; Sakuma et al., 2013). The  
341 presence of *HvHOX1* transcripts in central spikelets of two-rowed barleys, which are  
342 fertile and do not show any developmental disorder, poses a question that has yet to  
343 be solved (Komatsuda et al., 2007; Sakuma et al., 2010; Sakuma et al., 2013) (Fig.  
344 2C-F, Supplementary Fig. 7&8).

345 Following the comparison on spikelet initiation stages, we explored expression levels  
346 of these genes also in the spikelet growth stages of Bowman and BW-NIL(*vrs1.a*) (non-  
347 functional *HvHOX1*) by doing a quantitative real-time (qRT) PCR with tissue-unspecific  
348 (W5.0, W5.5, & W6.0) and tissue-specific (W7.5, W8.5, W10.0) samples (Fig. 3M-R).  
349 Also, in these later stages of development, *HvHOX1* exhibited significantly higher  
350 expression than *HvHOX2* in the whole spike at W5.0, W5.5, and W6.0, both in Bowman  
351 and BW-NIL(*vrs1.a*) (Fig. 3M & N). Intriguingly, *HvHOX1* displayed a reduced  
352 expression trend both in the central and lateral spikelets of Bowman from W7.5 to

353 W10.0 (Fig. 3O & Q). Contrastingly, *HvHOX2* had an increasing trend of expression in  
 354 these two tissues of Bowman (Fig. 3O & Q). More importantly, *HvHOX2* showed



355  
 356 **Figure 3: Two-rowed spikes have delayed and reduced lateral spikelet development compared to its central  
 357 and six-rowed lateral spikelets.**

358 Images of panel A & C are the W5.5 stage inflorescence meristem of six-rowed mutant BW-NIL(*vrs1.a*), and B & D  
 359 are from the two-rowed progenitor Bowman. Development of different organ primordia (AP, SP, CP, & GP) in central  
 360 spikelets (yellow color) of two-rowed (D) and six-rowed (C) are visibly similar. Awn primordium (AP) and carpel  
 361 primordium (CP) are formed only in lateral spikelets (blue color) of six-rowed (C) and not in two-rowed (D, marked  
 362 with red arrow heads). Cross sections of anthers and carpels of BW-NIL(*vrs1.a*) and Bowman are shown in E-L. The  
 363 W7.5 stage central spikelet anthers (E & G) and carpels (I & K) of BW-NIL(*vrs1.a*) and Bowman display normal  
 364 development, while the lateral spikelet anther (H) and carpel (L) of Bowman show suppressed and aborted  
 development. However, the lateral spikelet anther (F) and carpel (J) of BW-NIL(*vrs1.a*) seems developing normally  
 but comparatively slower than its central spikelet organs. Expression of *HvHOX1* and *HvHOX2* genes in the whole  
 spike (M & N), central spikelet (O & P), and lateral spikelet (Q & R) of Bowman and BW-NIL(*vrs1.a*) is shown,  
 respectively. In whole spike of W5.0 to W6.0 stages, *HvHOX1* expressed greater than *HvHOX2* both in Bowman (M)  
 and BW-NIL(*vrs1.a*) (N). Contrastingly, the *HvHOX2* showed stronger expression than *HvHOX1* in the Bowman  
 central spikelets of W7.5 to W10.0 (O); however, in BW-NIL(*vrs1.a*), *HvHOX2*'s expression was higher only in W8.5.  
 In the Bowman lateral spikelets of W7.5 to W10.0, *HvHOX1* and *HvHOX2* exhibited an anticyclic expression pattern,  
 i.e., when *HvHOX1*'s expression dropped down from W7.5 to W10.0, *HvHOX2*'s expression started increasing. Mean  
 values of M-R are compared with the multiple Student's *t*-test; \*, \*\*, \*\*\*, mean values are significantly different at 5, 1,  
 and 0.1% probability levels; ns-not significantly different. orange- stamen primordium; blue- carpel primordium; green:  
 glume primordium; pink: lemma primordium; purple: palea primordium; W-Waddington scale. Scale bar, A&B, 800  
 $\mu$ m; C&D, 200  $\mu$ m; E-L is 100  $\mu$ m.

365 greater expression than *HvHOX1* in the centrals (Fig. 3O), whereas in the laterals,  
366 *HvHOX1* had a superior level of expression in the first two stages (W7.5 and W8.5),  
367 followed by the increase of *HvHOX2* at W10.0 (Fig. 3Q). Crucially, the transcript levels  
368 of *HvHOX1* were gradually decreased from W7.5, while *HvHOX2* levels increased.  
369 Similar to the Bowman centrals, *HvHOX2* showed a higher trend of expression in BW-  
370 NIL(*vrs1.a*) central spikelets. However, the expression patterns of these two genes  
371 were different in BW-NIL(*vrs1.a*) lateral spikelets compared to Bowman (Fig. 3P & R).  
372 The antagonistic expression patterns of *HvHOX1* and *HvHOX2*, i.e., when *HvHOX2*  
373 expression goes up, *HvHOX1* expression turns down, suggests that these two genes  
374 might act anti-cyclic during the later growth stages. Based on this observation and the  
375 higher expression of *HvHOX2* (W7.5 to W10.0) in the Bowman central spikelets (Fig.  
376 3O) that show no developmental and growth aberration, we hypothesized that  
377 overexpression of *HvHOX2* might promote spikelet development by acting as a  
378 positive regulator of spikelet development.

379

380 **Promoters of *HvHOX1* and *HvHOX2* share similar spatiotemporal expression  
381 patterns during spike growth stages**

382 The expression studies of *HvHOX1* and *HvHOX2* (Fig. 2G-I & 3M-R) exemplified that  
383 these genes have similar temporal expression during the spikelet initiation and growth  
384 stages though at different amplitudes. Additionally, their central- and lateral-specific  
385 transcript levels indicated that they might also share spatial boundaries across the  
386 initiation and growth stages. To verify their spatial co-localization and similar temporal  
387 expression patterns, promoters (*HvHOX2*-1929 bp; *HvHOX1*-991 bp) of these genes  
388 were fused with a synthetic *GFP* (*GFP*) coding sequence and transformed into the two-  
389 rowed cv. Golden Promise. Five and eight independent transgenic events showed *GFP*  
390 accumulation in the  $T_0$  generation for *HvHOX1*, and *HvHOX2* *GFP* constructs,  
391 respectively. Three independent events from both the constructs were selected, and  
392 their *GFP* accumulation was confirmed until  $T_2$  generation. As expected, we found that  
393 promoter activity of these genes in identical tissues like the base of the central  
394 spikelet's carpel (Fig. 4A & D), the tapetal layer of the central spikelet's anther (Fig. 4B  
395 E), and rudimentary lateral anthers (Fig. 4C & F) at W8.5 stage. Collectively, the tissue-  
396 specific expression analysis and the promoter activity in the transgenic plants  
397 suggested that *HvHOX1* and *HvHOX2* might have similar spatiotemporal expression  
398 patterns during spikelet growth stages.

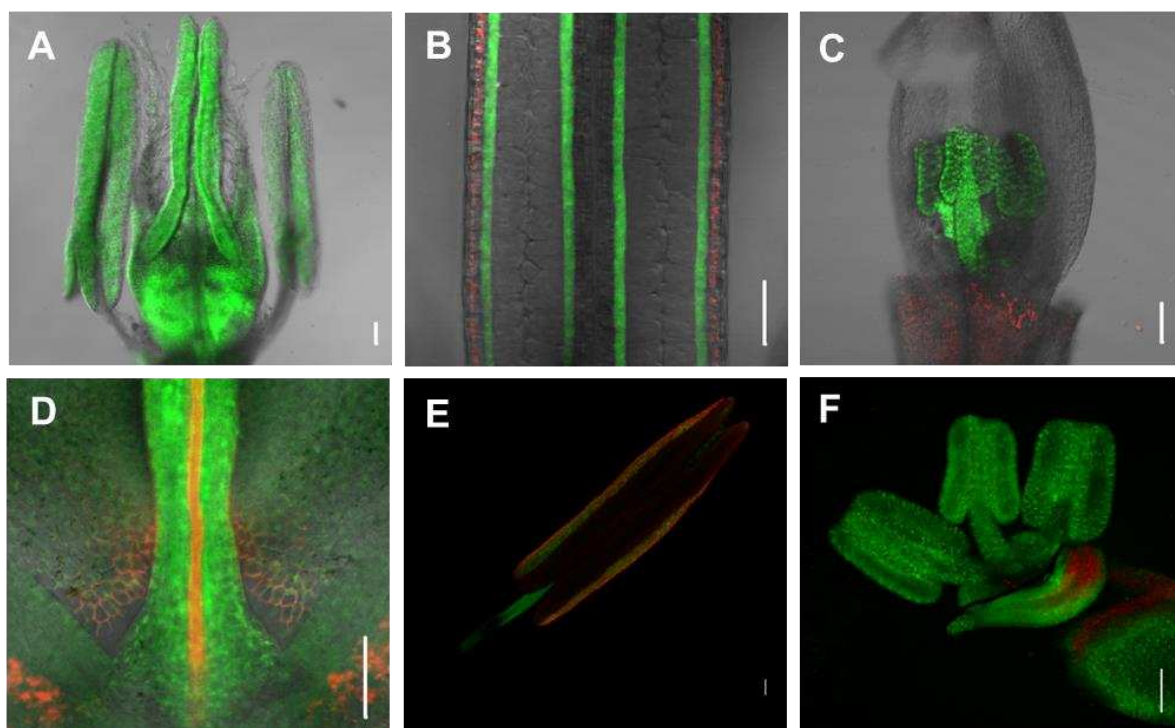


**Figure 4. *HvHOX1* and *HvHOX2* have similar spatiotemporal expression pattern during spike growth and development.**

*HvHOX2* promoter activity (GFP expression) in central spikelet's stamen and carpel (A), tapetum of central spikelet's stamen (B) and lateral spikelets' stamen (C) at W8.5 is shown. Similarly, *HvHOX1* promoter activity in central spikelets' carpel (D), tapetum of central spikelet's stamen (E) and lateral spikelet's stamen (F) is shown. Green color - GFP fluorescence; red color- chlorophyll autofluorescence. Scale bar 100  $\mu$ m. W- Waddington scale.

399 ***HvHOX1* has a unique co-expression module apart from a shared module with  
400 *HvHOX2* during spike development**

401 In an effort to predict the role of *HvHOX1* and *HvHOX2* genes, we constructed their  
402 co-expression signatures from the transcript profiles across six spikelet initiation and  
403 growth stages (W2.5, W3.0, W4.5, W6.5, W7.5, and W8.5) in Bowman. We found  
404 twenty co-expression modules from a set of 7,520 genes that showed a dynamic  
405 expression profile (Fig. 5A & B). *HvHOX1* and *HvHOX2* genes clustered together in  
406 one module (Figure 5A; red) along with 4,213 genes. A weighted gene co-expression  
407 network analysis (WGCNA) revealed that *HvHOX1* shares one part of its co-  
408 expression module (Fig. 5C, shown in blue, 16 genes) with *HvHOX2*, while *HvHOX1*  
409 has unique co-expressed signatures (Fig. 5C, shown in orange, 39 genes). Most  
410 importantly, *HvHOX2* is one of the co-expressed genes within the *HvHOX1* module  
411 (Fig. 5C). In other words, both genes share a similar expression signature across spike  
412 development. This supports our previous transcript and GFP analyses and suggests  
413 that these genes have similar spatiotemporal expression patterns. Furthermore,  
414 hierarchical clustering (HCL), divided the genes in the shared module (Supplementary

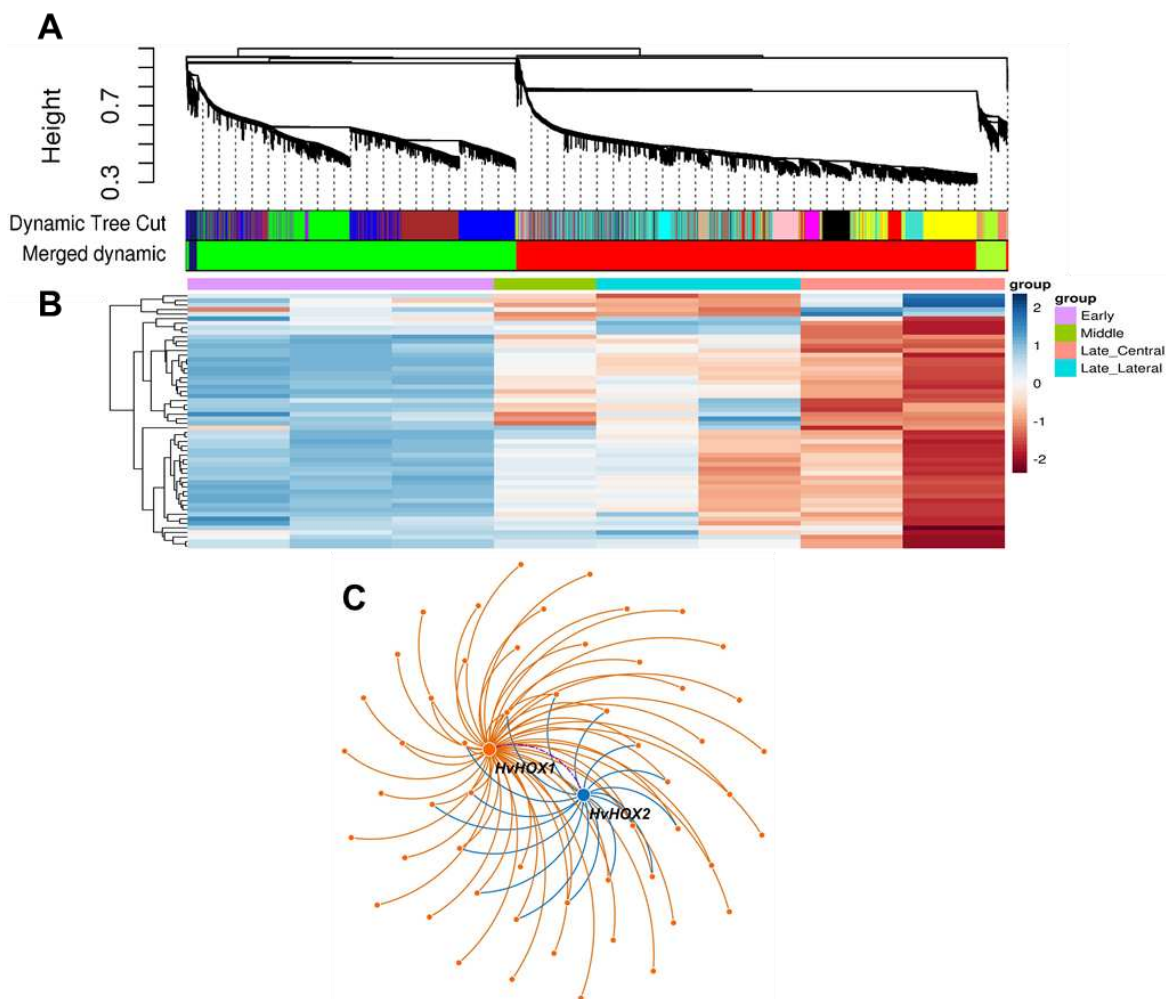


**Figure 5. Dendrogram from gene co-expression network analysis of two-rowed cv. Bowman spike tissues.** Modules of the co-expressed genes were assigned colors, shown by the horizontal bars below the dendrogram. Merged modules are shown under the dynamic module profile (A). Expression heat map of the red module is shown in (B) and the coexpressed gene clusters of *HvHOX1* and *HvHOX2* are shown in (C).

415 fig. 9A; blue) into two sub-clusters based on their expression in central and lateral  
416 spikelets, but not the unique *HvHOX1* co-expressed module (Supplementary Fig. 10B).  
417 This indicates that *HvHOX1* may play a specific role in the lateral spikelets, while  
418 *HvHOX2* probably has a different function from *HvHOX1*. Interestingly, the shared  
419 module was enriched with genes [e.g. *AGAMOUS* (*AG*), *SUPPRESSOR OF*  
420 *OVEREXPRESSION OF CONSTANS 1* (*SOC1*), *ENOLASE 1* (*ENO1*), and *AUXIN F-*  
421 *BOX PROTEIN 5* (*AFB5*)] associated with flower development, promotion of flowering,  
422 carpel and stamen identity, auxin signaling, transcription and nitrate assimilation  
423 (Covington and Harmer, 2007; Dreni and Kater, 2014; Hyun et al., 2016; Gaufichon et  
424 al., 2017). The *HvHOX1* unique co-expressed module, on the other hand, was  
425 enriched in genes [such as *BREVIPEDICELLUS 1* (*BP1*), *WRKY 12*, *NOVEL PLANT*  
426 *SNARE 11* (*NPSN11*), *FORMIN HOMOLOGY 14* (*AFH14*), *LONELY GUY 3* (*LOG3*),  
427 and *G PROTEIN ALPHA SUBUNIT 1* (*GPA1*)] that are predicted to be involved in

428 inflorescence architecture, flower development, ABA response, cell division, cell  
 429 communication, senescence, and cell death (Li et al., 2010; Tokunaga et al., 2012;  
 430 Zhao et al., 2015; Li et al., 2016; Chakraborty et al., 2019; Wu et al., 2020)  
 431 (Supplementary Table 4).

432  
 433 **HvHOX2 might be a dispensable gene during barley spikelet development**  
 434 To understand the function of *HvHOX2*, we developed *Hvhox2* mutants by using RNA-  
 435 guided Cas9 endonucleases (RGEN). A guide RNA was designed for the conserved

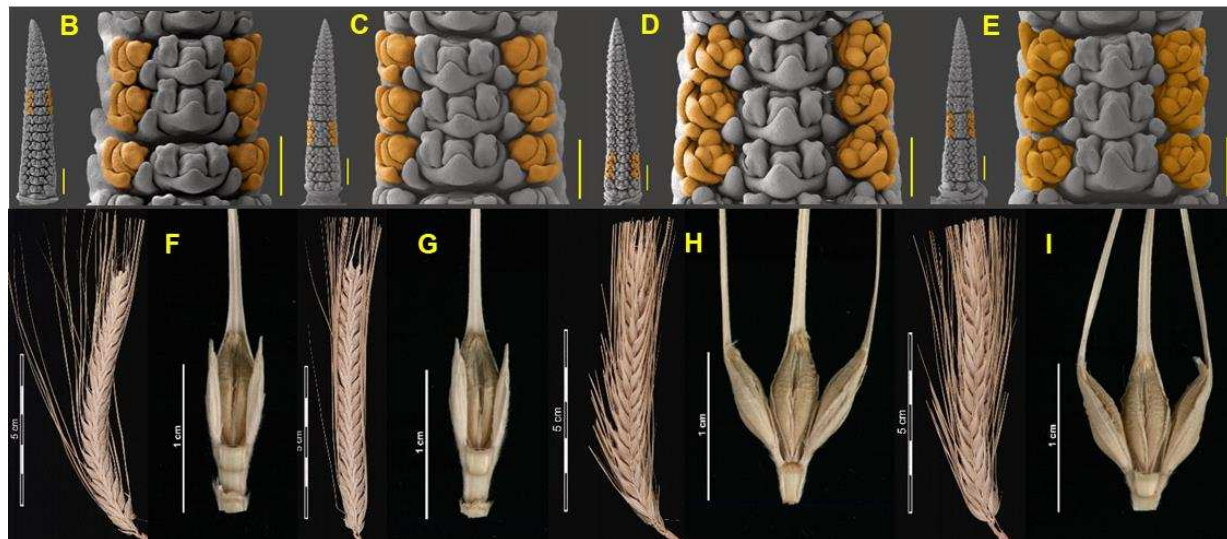
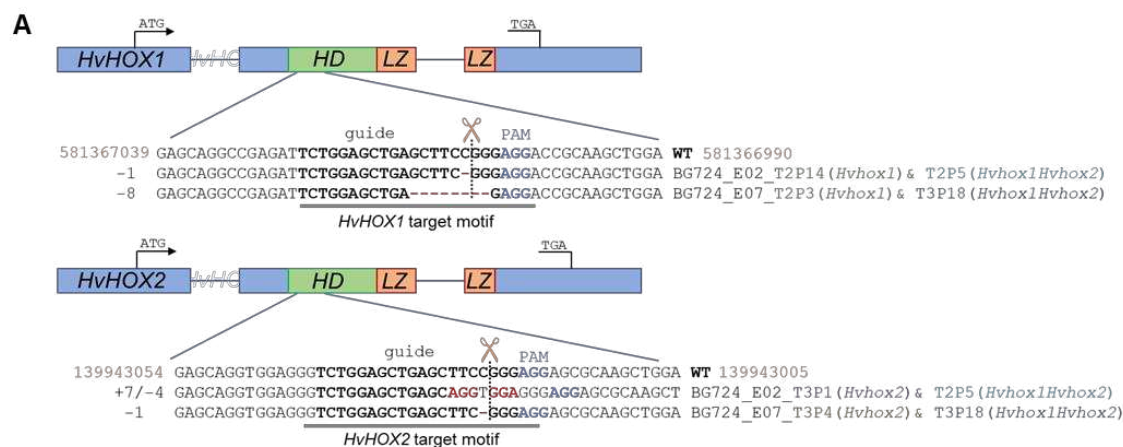


**Figure 6: *HvHOX2* gene might be a team player in barley spikelet development.** Figure A graphically shows the guide sequence with the Protospacer Adjacent Motif (PAM) and a putative cutting site, used to generate the single and double mutants of *HvHOX1* and *HvHOX2* genes, by using Cas9 endonuclease. Figures B & F are from an azygous plant and C-D & G-I are the representative images of the BG724-E07 mutants. Figures B-E compare the lateral spikelet development of wild-type, single and double mutants of *HvHOX1* and *HvHOX2* genes. At W4.5, the lateral spikelet primordia of *HvHOX2* mutant (C) is at similar developmental stage with the wild-type (B) by having differentiated primordia for only glume and lemma. However, the mutant of *HvHOX1* (D) and double mutant of *HvHOX1* and *HvHOX2* (E) displayed an advanced lateral spikelet development with the well differentiated primordia for glume, lemma, stamen, and carpel. The matured lateral spikelets of *HvHOX2* mutant (G) and wild-type (F) are sterile and smaller compared to the fertile lateral spikelets that form grains of *HvHOX1* mutant (H) and *HvHOX1* and *HvHOX2* double mutant (I). Scale bar-whole spikes in B, C, D, & E, 500  $\mu$ m; magnified three nodes, 200  $\mu$ m; HD-Homeodomain; LZ-Leucine Zipper.

436 homeodomain region shared by *HvHOX1* and *HvHOX2* for site-directed mutagenesis  
437 of both genes (Fig. 6A). We created the mutants in the two-rowed cv. Golden Promise,  
438 via stable transformation, using respective constructs and identified the independent  
439 events BG724\_E02 and BG724\_E07 bearing different insertions and/or deletions by  
440 sequencing their target regions. Among the progenies of these primary  
441 (heterozygous/chimeric) mutants, wild-type (T-DNA-free, non-mutant) plants, as well  
442 as single and double mutants for both genes, were selected (Fig. 6A). For *HvHox1*, the  
443 two mutants, BG724\_E02 and BG724\_E07, had one and eight nucleotides deletions,  
444 respectively, in the target regions (Fig. 6A), which created two frame shifted mutant  
445 *HvHOX1* proteins (Supplementary Fig. 10A&B). With regards to *Hvhox2*, the  
446 BG724\_E02 event had seven nucleotides addition and four nucleotides deletion (Fig.  
447 6A), which resulted in a mutant *HvHOX2* protein that had one amino acid addition and  
448 one amino acid exchange in the first HD (Supplementary Fig. 10C). Similar to the  
449 *Hvhox1* BG724\_E02 mutant, *Hvhox2* BG724\_E07 mutant possessed one nucleotide  
450 deletion (Fig. 6A) and formed a frame shifted protein (Supplementary Fig. 10D). The  
451 spikelet development of these plants was compared at W4.5 and after spike maturity.  
452 It was found that the central and lateral spikelets of the *Hvhox2* mutants (Fig. 6C,  
453 Supplementary Fig. 11B) displayed a similar stage of differentiation at W4.5 as in the  
454 spikes of wild-type plants (Fig. 6B, Supplementary Fig. 11A). Analogous to the pattern  
455 of spikelet differentiation, the matured spikes of *Hvhox2* mutants (Fig. 6G,  
456 Supplementary Fig. 11F) possessed smaller (compared to the centrals) and sterile  
457 lateral spikelets like in spikes of wild-type plants (Fig. 6F, Supplementary Fig. 11E),  
458 implying that *HvHOX2* might neither promote nor suppress spikelet primordia  
459 differentiation and growth. However, *Hvhox1* single (Fig. 6D, Supplementary Fig. 11C)  
460 and double mutants (*Hvhox1/Hvhox2*) (Fig. 6E, Supplementary Fig. 11D) exhibited  
461 advanced lateral spikelet differentiation compared to wild-type plants (Fig. 6B,  
462 Supplementary Fig. 11A) and *Hvhox2* mutants (Fig. 6C, Supplementary Fig. 11B).  
463 Interestingly, the lateral spikelet differentiation of *Hvhox1* (Fig. 6D, Supplementary Fig.  
464 11C) and double mutants (*Hvhox1/Hvhox2*) (Fig. 6E, Supplementary Fig. 11D) were  
465 at a similar stage at W4.5, which reiterated the fact that *HvHOX1* is suppressing lateral  
466 spikelet development in two-rowed spikes, irrespective of the *HvHOX2* function. As  
467 expected, spikes of *Hvhox1* single (Fig. 6H, Supplementary Fig. 11G) and double  
468 mutant (*Hvhox1/Hvhox2*) (Fig. 6I, Supplementary Fig. 11H) had bigger and fertile  
469 spikelets (grains) like six-rowed barley. We explored *Hvhox2* mutants by screening its

470 coding sequence in 5500 second-generation (M<sub>2</sub>) TILLING (Targeting Induced Local  
471 Lesions in Genomes) mutant lines of cv. Barke (Gottwald et al., 2009), and found only  
472 four mutations. Among these, three were synonymous, and one was non-synonymous  
473 (P197S, line 11869) nucleotide substitutions (Supplementary Fig. 12). Interestingly,  
474 the mutant line 11869 did not show aberrations during spike development and growth  
475 in the M<sub>3</sub> generation, which supported our RGEN *Hvhox2* mutants. Taken together,  
476 our RGEN mutant analyses suggest that *Hvhox2*, at its native expression level,  
477 appears dispensable for barley spikelet development.

478

#### 479 **Overexpression of *Hvhox2* can promote lateral spikelet development**

480 Our qRT expression study conducted during spike growth stages revealed that higher  
481 transcript levels of *Hvhox2* than *Hvhox1* in central spikelets might be associated with  
482 the proper development of those spikelets in two-rowed barley (Fig. 3D, G, K & O). To  
483 validate this '*Hvhox2*-dosage'-hypothesis, we tagged the *Hvhox1* promoter (991 bp  
484 – also used for assessing the spatiotemporal activity of *Hvhox1* promoter) with the  
485 coding sequence of *Hvhox2* and used these constructs to create transgenic plants of  
486 cv. Golden Promise. We used the *Hvhox1* promoter because *Hvhox1* expresses  
487 higher in the lateral spikelets (Supplementary Fig. 8B, Fig. 3Q), so this promoter might  
488 increase the transcript levels of *Hvhox2* in the lateral spikelets of transgenic plants.  
489 As a result, the smaller and sterile lateral spikelets might be restored to fertile and  
490 bigger spikelets. Eight independent transgene-positive events were selected and  
491 screened for the restored lateral spikelets. Two events, E189 (at T<sub>2</sub>) and E541 (at T<sub>1</sub>),  
492 showed partial promotion of lateral spikelets compared to a wild-type control plant  
493 E511 (Fig. 7). The spikes of the two events displayed an advanced lateral spikelet  
494 differentiation at W4.5 compared to the spike of wild-type (E511) plants (Fig. 7A-C).  
495 Interestingly, the lateral spikelets of both the events had a quantitative difference in  
496 development, in which E189 showed a mild promotion, while E541 possessed a bit  
497 stronger improvement compared to the spikes of control plants (Fig. 7B & C). The  
498 matured spikes of E189 and E541 had partially restored lateral spikelets that are bigger  
499 and occasionally developed small awns in contrast to the spikes of control plants (Fig.  
500 7D-F). The matured lateral spikelets of E189 were smaller than E541, which followed  
501 the similar pattern of developmental differentiation observed during spikelet  
502 differentiation (Fig. 7B&C and E&F). Then, we quantified the transcripts of *Hvhox1*,  
503 *Hvhox2*, and *Hvhox2-T* (*Hvhox1pro::Hvhox2*) in W6.5 (tissue-unspecific) (Fig.

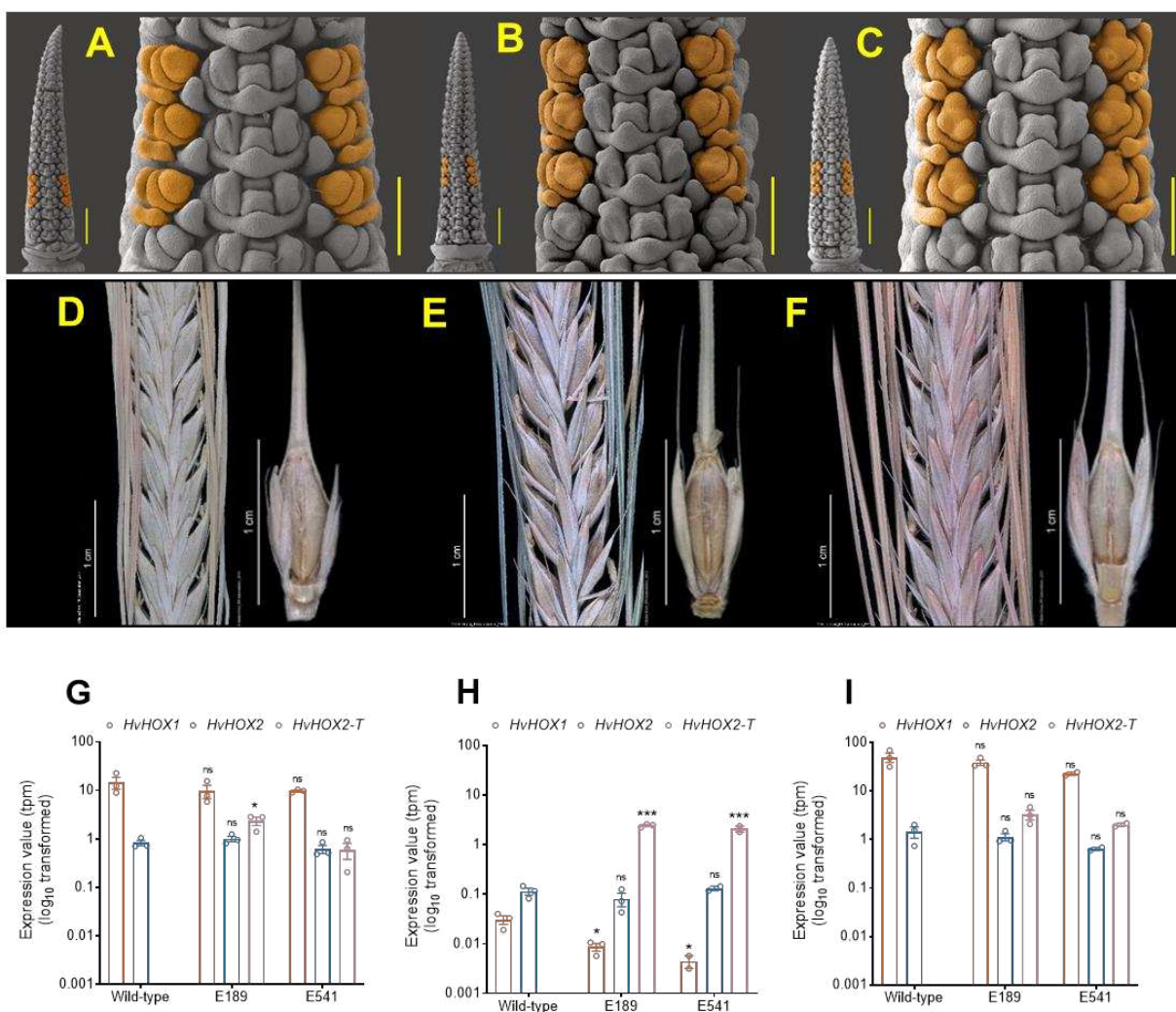


**Figure 7: Overexpression of *HvHOX2* partially restored the lateral spikelet development in two-rowed barley.** A comparison of wild-type (A) and two transgenic plants E189 (B) E541 (C) lateral spikelet primordia differentiation is displayed. The lateral spikelet primordia of transgenic plants E189 and E541 exhibited an advanced development compared to the wild-type at W4.5. At this stage, the wild-type laterals are found only with the differentiated glume and lemma primordia, while both the transgenic plants already initiated three stamen primordia along with the glume and lemma primordia. Matured spikes and triple spikelets of wild-type (D), E189 (E), and E541 (F) are shown. The lateral spikelets of both the transgenic plants are bigger compared to the wild-type and occasionally found with short awns. Quantification of endogenous *HvHOX1* and *HvHOX2* and transgenic *HvHOX2-T* expression performed in a wild-type and two independent transgenic plants' (E189 & E541) whole spike at W6.5 (G), central spikelet (H) and lateral spikelets (I) at W8.0 is shown. The overexpression of transgenic *HvHOX2-T* did not greatly change the endogenous *HvHOX1* and *HvHOX2* expression in the whole spike at W6.5 (G) and lateral spikelets of W8.0 (I). However, in the central spikelets of W8.0, the transgenic *HvHOX2-T* expression drastically lowered the *HvHOX1* expression (H). In G, H & I, the mean values of *HvHOX1* from the transgenic plants were compared to the wild-type. Similarly, both the endogenous and transgenic *HvHOX2* of transgenic plants were compared with the wild-type *HvHOX2* expression. Mean values of G-I are compared with the multiple Student's *t*-test; \*, \*\*, mean values are significantly different at 5 and 0.1% probability levels. In A, B, & C, the scale bars of whole spike images represent 500  $\mu$ m, and in magnified three node images they represent 200  $\mu$ m. W-Waddington scale.

504 7G) and W8.0 (tissue-specific) (Fig. 7H&I). It revealed that both the events (E189 &  
 505 E541) had *HvHOX2-T* transcripts in the two stages and tissues analyzed (Fig. 7G-I).  
 506 Most importantly, there was no difference in the expression levels of *HvHOX1* and  
 507 *HvHOX2* genes in the lateral spikelets of transgenic events compared to the azygous  
 508 plant (Fig. 7I). However, we found a significant reduction of *HvHOX1* transcripts in the

509 central spikelets (Fig. 7H). We also observed that event E189 had a four-fold higher  
510 expression of *HvHOX2-T* than E541 at W6.5 (Fig. 7G), which was similarly seen in the  
511 lateral spikelets at W8.0, where E189 had 1.6-fold higher expression than E541 (Fig.  
512 7I). We hypothesize that this difference in expression is mainly due to the  
513 developmental disparity between E189 and E541 (Fig. 7B & C). Thus, our  
514 overexpression study supports the idea that increasing the dosage of *HvHOX2*  
515 transcripts promotes lateral spikelet development in two-rowed barley.

516

## 517 Discussion

### 518 ***HvHOX1* and *HvHOX2*, two functional HD-ZIP class I transcription factors, may 519 act antagonistically to each other**

520 Based on the sequence similarity of *HvHOX2* to its orthologs in grass species, it was  
521 proposed that *HvHOX2* might have a similar molecular role in the Poaceae (Sakuma  
522 et al., 2010). However, *HvHOX1*, specific to the Triticeae tribe, showed a very high  
523 sequence variation, at least in barley (Komatsuda et al., 2007; Saisho et al., 2009;  
524 Casas et al., 2018). It was hypothesized that *HvHOX1* and *HvHOX2* are duplicated  
525 genes, in which *HvHOX2* might be retaining the ancestral sequence and promotion of  
526 development, while *HvHOX1* became neofunctionalized as a suppressor of lateral  
527 spikelets (Sakuma et al., 2010; Sakuma et al., 2013). Our nucleotide diversity study  
528 also supports this postulation, as we found a higher nucleotide diversity for *HvHOX1*  
529 than *HvHOX2* (Supplementary Fig. 1, Supplementary Table 3). Despite a few amino  
530 acid changes between *HvHOX1* and *HvHOX2* proteins (Supplementary Fig. 3), both  
531 of them can bind to their HD-ZIP class I-specific cis-element, make dimers, and  
532 transactivate their downstream genes (Fig. 1, Supplementary Fig. 3&4), thus  
533 confirming that both are functional HD-ZIP class I TFs. Also, our expression studies  
534 suggested that both the genes have similar spatiotemporal expression patterns during  
535 spikelet initiation (Fig. 2) and growth stages (Fig. 3 & 4) that could facilitate the  
536 interaction between them. Similarly, our gene co-expression network (GCN) analysis  
537 revealed that most likely, these genes are sharing similar gene networks, as they fall  
538 into the same cluster of co-expressed genes and share a common network of genes  
539 (Fig. 5). This finding reaffirms the hypothesis that both genes might have originated  
540 from a common ancestral gene (Sakuma et al., 2010; Sakuma et al., 2013). Crucially,  
541 *HvHOX1* has a unique network of genes (Fig. 5C) that are highly expressed in lateral  
542 spikelets (Supplementary Fig. 9B) and are enriched with genes that are involved in the

543 suppression of development and exert cell death (Supplementary Table 4)  
544 (Thirulogachandar et al., 2017). It also corroborates that *HvHOX1* might have acquired  
545 a new role as a suppressor of lateral spikelets in barley. Contrastingly, the genes in  
546 the shared network of *HvHOX1* and *HvHOX2* are expressed both in the central and  
547 lateral spikelets, and they are predicted to function towards the promotion of  
548 development and flowering. It also suggests that along with the suppressors, there  
549 might also be some promoters that are highly expressed in the lateral spikelets.  
550 Presumably, this is the first insight into the antagonistic behavior of these two genes  
551 during barley spikelet development.

552 Additionally, our analyses of differentially expressed genes between Bowman and BW-  
553 NIL(*vrs1.a*) (Supplementary Fig. 13&14) and wild-type and *HvHOX2* overexpressing  
554 transgenic plants (Supplementary Fig. 15) pointed out that *HvHOX1* and *HvHOX2*  
555 might work antagonistically to each other during spikelet development. There are many  
556 examples in plants in which homologous/paralogous genes are antagonists. In  
557 *Arabidopsis*, *WRKY12* and *WRKY13* oppositely modulate flowering time under SD  
558 conditions; *WRKY12* promotes flowering, whereas *WRKY13* delays this process (Li et  
559 al., 2016). Likewise, *TERMINAL FLOWER 1* (*TFL1*) and *FLOWERING LOCUS T* (*FT*)  
560 are homologous PEBP class proteins, which are antagonistic to each other; *TFL1*  
561 being a repressor and *FT* an activator of flowering (Hanzawa et al., 2005). Another  
562 example is the closely related MADS-box proteins *SHORT VEGETATIVE PHASE*  
563 (*SVP*) and *AGAMOUS-LIKE 24* (*AGL24*), which perform opposite roles during the floral  
564 transition, acting as repressor and promotor of flowering, respectively (Hartmann et al.,  
565 2000; Yu et al., 2002; Michaels et al., 2003; Lee et al., 2007). Recently, in rice, it was  
566 found that *Teosinte branched 2* (*Tb2*) counteracts with its paralog *Tb1* to influence tiller  
567 number(Lyu et al., 2020). All these instances corroborate that gene duplication events  
568 followed by neofunctionalization might generate homologous/paralogous genes that  
569 can act antagonistically to each other and modulate specific developmental pathways.  
570 To understand the evolutionary importance of these genes, a new sub-category under  
571 neofunctionalization might be necessary for which we propose to group them as  
572 'antifunctionalized' homologs. Thus, our studies suggest that the paralogous HD-ZIP  
573 class I transcription factors, *HvHOX1*, and *HvHOX2* are antifunctionalized and may act  
574 against each other during barley spikelet development.

575

576

577 **Dosage of *HvHOX1* and *HvHOX2* transcripts influence spikelet development**

578 *HvHOX1* was previously proposed as a negative regulator of lateral spikelet,  
579 specifically pistil/carpel development, in barley (Komatsuda et al., 2007; Sakuma et al.,  
580 2010; Sakuma et al., 2013). We found evidence supporting the claim that from the  
581 initiation of TM (Fig. 2G & H) to W8.5 (Fig. 3M & Q), *HvHOX1* transcripts are enriched  
582 in the lateral spikelets of two-rowed barley. This correlated well with the delayed  
583 meristem differentiation (Fig. 2B-F) and anther and carpel development within the  
584 lateral spikelets (Fig. 3E-L, Supplementary Fig. 6&7). More importantly, the abortion of  
585 lateral spikelets' anther and pistil/carpel at W7.5 (Fig. 3E-L, Supplementary Fig. 6&7),  
586 and the gradual reduction of *HvHOX1* expression in lateral spikelets from W7.5 (Fig.  
587 3Q), reaffirm that *HvHOX1* is highly expressed in the reproductive organs of lateral  
588 spikelets. We also identified *HvHOX1* transcripts in central spikelets during early and  
589 late spikelet development (Fig. 2H; Fig. 3O & Q). However, we observed no disorder  
590 during spikelet differentiation (Fig. 2B-F, 3C & D) or growth of reproductive organs (Fig.  
591 3E-L, Supplementary Fig. 6&7) in two-rowed barley. Also, previous studies did not  
592 report any developmental irregularities in central spikelets of two-rowed barley  
593 (Komatsuda et al., 2007; Sakuma et al., 2010; Sakuma et al., 2013; Zwirek et al.,  
594 2019). We, therefore, hypothesized that this could be due to a lower dosage of  
595 *HvHOX1* transcripts (compared to the laterals) (Fig. 2H & 3O) and some more positive  
596 regulators, which act antagonistically to *HvHOX1* in central spikelets. It led us to  
597 examine the expression of *HvHOX2* - a paralog of *HvHOX1*, which was proposed to  
598 be promoting the development in barley (Sakuma et al., 2010; Sakuma et al., 2013). A  
599 similar (i.e., non-significant) level of *HvHOX2* transcripts as *HvHOX1* during the early  
600 spikelet differentiation stages (Supplementary Fig. 8A) (except at SP stage), and a  
601 higher dosage of *HvHOX2* transcripts in the central spikelets across the growth of  
602 reproductive organs (Fig. 3O) supports the claim of a promoting *HvHOX2* function.  
603 Furthermore, we recognized an anti-cyclic expression pattern between these two  
604 genes during the growth stages (Fig. 3Q) and binding of *HvHOX1* protein on *HvHOX2*  
605 promoter and vice versa (Supplementary Fig. 4) indicating that these genes influence  
606 the expression pattern of each other. A similar expression pattern of these two genes  
607 had already been reported in other two-rowed barleys (Sakuma et al., 2013).  
608 Our RGEN mutant study suggests that *HvHOX2* is rather dispensable during barley  
609 spikelet development because the two *Hvhox2* mutants retained a canonical spikelet  
610 development in laterals and centrals of wild-type plants (Fig. 6, Supplementary Fig.

611 10). Interestingly, ubiquitous overexpression of orthologous *HOX2* genes in  
612 wheat(Wang et al., 2017) and rice(Shao et al., 2018) reduced the inflorescence length  
613 and complexity. However, when *HvHOX2* transcripts were increased transgenically,  
614 *HvHOX2* can restore and promote barley lateral spikelet development in a dosage-  
615 dependent manner (Fig. 7). A significant reduction of *HvHOX1* transcripts in the central  
616 spikelets of *HvHOX2* overexpression mutants (Fig. 7H) reinstated that these two genes  
617 can influence each other's expression level. We also observed a reduction of *HvHOX1*  
618 transcripts in the lateral spikelets of *HvHOX2* overexpression plants. Specifically, 3.5  
619 and 6.9 times (mean transcript values) of reduction in transcripts were identified in the  
620 *HvHOX2* overexpressing plants E189 and E541, respectively; however, the declines  
621 were not statistically significant (Fig. 7I). We hypothesize that this could be due to the  
622 solid lateral-specific expression of *HvHOX1*, which is under the control of VRS4  
623 (*HvRA2*) and VRS3 – two upstream regulators of *HvHOX1* (Koppolu et al., 2013;  
624 Sakuma et al., 2013; Bull et al., 2017; van Esse et al., 2017). The reduction level of  
625 *HvHOX1* transcripts and the degree of lateral spikelet promotion in the two *HvHOX2*  
626 overexpression events indicated that *HvHOX1* regulates lateral spikelet development  
627 based on the dosage of its expression, which was also shown previously (Sakuma et  
628 al., 2013). Taken together, our expression and transgenic studies suggest that the  
629 transcript levels of *HvHOX1* and *HvHOX2* influence lateral spikelet development in  
630 two-rowed barley in a dosage-dependent fashion.

631

## 632 **Methods:**

### 633 **Plant materials and their growth conditions**

634 Barley cultivars, Bonus, Bowman, and Golden Promise, were used in this study as two-  
635 rowed representatives and induced mutant *hex-v.3* (progenitor cv. Bonus), cultivar  
636 Morex and Bowman backcross-derived line BW-NIL(*vrs1.a*) / BW 898 (Druka et al.,  
637 2011) were used as six-rowed representatives. Wild species of *Hordeum* were  
638 obtained from Dr. Roland von Bothmer, Swedish University of Agricultural Sciences,  
639 Alnarp, Sweden (Supplementary table 2). *Arabidopsis thaliana* Col-0 plants were used  
640 for protoplast isolations and grown on a 1:3 vermiculite: soil mixture in a phytochamber  
641 (8 hr light/16 hr dark at 20° C and 18° C, respectively; 60 % humidity). See the  
642 supplemental methods for detailed information.

643

644

645 **Microscopic studies**

646 Please refer to the supplementary experimental procedures for histology of anther,  
647 carpel, and spike development, as well as different microscopic methods like light,  
648 scanning electron, and fluorescence.

649

650 **Nucleic acid analysis**

651 In the Supplemental methods, one can find methods for genomic DNA extraction,  
652 Southern hybridization, RNA extraction, and qRT-PCR.

653

654 **Nucleotide diversity ( $\pi$ ) calculation**

655 The whole-genome resequencing (WGS) data and SNP matrix for 200 diverse barley  
656 genotypes were downloaded from Jayakodi et al., 2020. The sequencing reads were  
657 aligned to the reference cv. Morex, as described (Jayakodi et al., 2020). The effectively  
658 covered areas of the barley genome were identified by the regions covered by at least  
659 two reads in  $\geq 80\%$  of the WGS accessions. The nucleotide diversity ( $\pi$ ) was calculated  
660 on a 10 kb window with a step size of 2 kb with a custom script. Only the windows with  
661  $\geq 2$  kb effectively covered region were considered. Please refer to the Supplemental  
662 methods for further nucleotide diversity analyses, including TILLING and resequencing  
663 of *HvHOX1* and *HvHOX2* in various genotypes and species.

664

665 **Microarray probe preparation and data analysis**

666 The microarray probe preparation, hybridization, and data analysis were done as  
667 previously reported (Thirulogachandar et al., 2017). An elaborate method of the data  
668 preparation and co-expression network construction is given in the supplemental  
669 methods

670

671 **Data analysis**

672 The qRT data were analyzed using the Prism software, version 8.4.2 (GraphPad  
673 Software, LLC). Mean value comparison of different traits was made with the multiple  
674 Student's t-tests, paired Student's t-test (parametric), and a one-way ANOVA with  
675 Tukey's multiple comparison test (alpha=5%).

676

677

678

679 **Gene ontology enrichment analysis**

680 The Gene Ontology (GO) enrichment analysis of differentially expressed genes and  
681 gene modules was done using the agriGO platform (v2) (Tian et al., 2017). The  
682 selected genes' Arabidopsis IDs were queried against the Arabidopsis genome locus  
683 (TAIR9) reference set with the Fisher statistical test, Hochberg (FDR) multi-test  
684 adjustment method, and a significance level 0.05. The Plant GO slim "GO type" has  
685 been selected with a minimum number of entries. For final interpretation, the GO  
686 enrichment of biological processes was used.

687

688 **Transgenic and targeted mutagenesis**

689 *In silico* identification of genes and promoters used for generating the transgenic plants  
690 used in this study are given in the Supplemental methods. Also, the methods of cloning  
691 various constructs, guide RNA design and preparation Cas9-triggered mutagenesis,  
692 as well as plant transformation are shown in the supplemental methods.

693

694 **Analysis of proteins**

695 The preparation details of constructs used for the transactivation assay, electrophoretic  
696 mobility shift assay (EMSA), Western blot, and bimolecular fluorescence  
697 complementation assay are given in the supplemental methods.

698

699 **Author Contributions**

700 V.T., N.S., T.S. G.G., and T.K. conceptualized the study. The study was supervised by  
701 N.S., T.S., and M.K. Microscopic analyses were done by V.T., and T.R. Transcriptome  
702 data were generated by V.T., and G.G., which was analyzed by V.T., and S.K.  
703 Transgenics and targeted gene-specific mutants were generated by G.H. and J.K. and  
704 analyzed by V.T. RGEN mutants were molecularly characterized by J.R.  
705 Resequencing of genes, and TILLING analysis were performed by R.K., T.S., S.S.,  
706 T.K., and M.J. Constructs for protein characterization were prepared by G.G., V.T.,  
707 P.S.R., and C.S. Transactivation and BiFC experiments were conducted by L.E-L.,  
708 G.G., and J.L., and M.K. performed DNA binding study (EMSA). All the data were  
709 compiled, interpreted and drafted by V.T. The manuscript was reviewed by all the  
710 authors.

711

712

713 **Acknowledgments**

714 We express our sincere gratitude to Jana Lorenz, Mandy Püffeld, Gabi Einert, Corinna  
715 Trautewig, and Angelika Püschel for their excellent technical support. We would like to  
716 thank Karin Lipfert, Heike Müller, Gudrun Schütze and Andreas Bähring for  
717 photography and graphical works. We are grateful to Sabine Sommerfeld und Sibylle  
718 Freist for technical assistance in barley transformation. We also extend our thanks to  
719 Dr. Nils Stein for providing access to TILLING screening platform and Stefan Ortaleb for  
720 creating the spike movie. Work in the N.S. laboratory has been supported by a grant  
721 from the Ministry of Education Saxony-Anhalt (IZN), while work in the T.S. laboratory  
722 has been supported by the HEISENBERG Program of the German Research  
723 Foundation (DFG), grant nos. SCHN 768/8-1 and SCHN 768/15-1 and the IPK core  
724 budget.

725

726 **Competing interests**

727 The authors declare no competing interests.

728

729 **Accession number**

730 *HvHOX1 (VRS1)* (Version: AB259782.1, GI: 119943316)

731 *HvHOX2* (Version: AB490233.1, GI: 266265607)

732

733 **Supplemental data**

734 Supplemental Figure S1: Comparison of HvHOX1 and HvHOX2 nucleotide diversity  
735 in 200 domesticated barleys

736 Supplemental Figure S2: Pairwise alignment of HvHOX1 and HvHOX2 proteins

737 Supplemental Figure S3: Western blot for HvHOX1 and HvHOX2 proteins

738 Supplemental Figure S4: EMSA competition assay of in vitro translated HvHOX1 and  
739 HvHOX2

740 Supplemental Figure S5. Two-rowed spikes have delayed lateral spikelet  
741 development compared to its central spikelet and six-rowed lateral spikelets

742 Supplemental Figure S6. Transverse sections of anthers from central and lateral  
743 spikelets of Bowman and BW-NIL(vrs1.a)

744 Supplemental Figure S7: Transverse sections of carpels from central and lateral  
745 spikelets of Bowman and BW-NIL(vrs1.a)

746 Supplemental Figure S8: Comparison of HvHOX1 and HvHOX2 expression pattern  
747 during early spike development

748 Supplemental Figure S9. Hierarchical clustering of HvHOX1 and HvHOX2 shared and  
749 HvHOX1 unique modules

750 Supplemental Figure S10: Sequence alignment of the wild-type and mutant proteins  
751 of HvHOX1 and HvHOX2 resulted from the RGEN study

752 Supplemental Figure S11: The HvHOX2 gene might be a team player in barley  
753 spikelet development

754 Supplemental Figure S12: Multiple sequence alignment of the orthologous HvHOX2  
755 proteins and HvHOX2 from a TILLING mutant 11869

756 Supplemental Figure S13. Gene ontology of Differentially expressed genes in W2.5,  
757 W3.0 and W4.5 in Bowman and BW-NIL(vrs1.a).

758 Supplemental Figure S14. Gene ontology of differentially expressed genes in W7.5  
759 and W8.5 lateral spikelets of Bowman.

760 Supplemental Figure S15. Gene ontology of differentially expressed genes in W8.0  
761 lateral spikelets of Transgenic plant E189 vs control plant E511.

762 Supplemental Methods. Additional methods and analyses used in this study.

763 Supplemental Table S1. HvHOX2 SNP haplotypes identified in 83 diverse spring  
764 barley collection

765 Supplemental Table S2. List of *Hordeum* species used in this study.

766 Supplemental Table S3. Nucleotide diversity of *HvHOX1* and *HvHOX2* in *Hordeum*  
767 species.

768 Supplemental Table S4. List of genes coexpressed with HvHOX1 and HvHOX2  
769 genes during spike development in cv. Bowman

770 Supplemental Table S5. Primers used in this study.

771

772

773 **References**

774 Arce, A.L., Rainieri, J., Capella, M., Cabello, J.V., and Chan, R.L. (2011).  
775 Uncharacterized conserved motifs outside the HD-Zip domain in HD-Zip  
776 subfamily I transcription factors; a potential source of functional diversity. *BMC*  
777 *Plant Biol* 11, 42.

778 Ariel, F.D., Manavella, P.A., Dezar, C.A., and Chan, R.L. (2007). The true story of the  
779 HD-Zip family. *Trends Plant Sci* 12, 419-426.

780 Bonnett, O.T. (1935). The development of the barley spike. *Journal of Agricultural*  
781 *Research* 51, 451-457.

782 Bull, H., Casao, M.C., Zwirek, M., Flavell, A.J., Thomas, W.T.B., Guo, W.B., Zhang,  
783 R.X., Rapazote-Flores, P., Kyriakidis, S., Russell, J., Druka, A., McKim, S.M.,  
784 and Waugh, R. (2017). Barley SIX-ROWED SPIKE3 encodes a putative Jumonji  
785 C-type H3K9me2/me3 demethylase that represses lateral spikelet fertility. *Nat*  
786 *Commun* 8.

787 Capella, M., Re, D.A., Arce, A.L., and Chan, R.L. (2014). Plant homeodomain-leucine  
788 zipper I transcription factors exhibit different functional AHA motifs that  
789 selectively interact with TBP or/and TFIIB. *Plant Cell Rep* 33, 955-967.

790 Casas, A.M., Contreras-Moreira, B., Cantalapiedra, C.P., Sakuma, S., Gracia, M.P.,  
791 Moralejo, M., Molina-Cano, J.L., Komatsuda, T., and Igartua, E. (2018).  
792 Resequencing the Vrs1 gene in Spanish barley landraces revealed reversion of  
793 six-rowed to two-rowed spike. *Molecular Breeding* 38, 51.

794 Chakraborty, N., Kanyuka, K., Jaiswal, D.K., Kumar, A., Arora, V., Malik, A., Gupta, N.,  
795 Hooley, R., and Raghuram, N. (2019). GCR1 and GPA1 coupling regulates  
796 nitrate, cell wall, immunity and light responses in *Arabidopsis*. *Sci Rep-Uk* 9, 1-  
797 17.

798 Clifford, H., Soderstrom, T., Hilu, K., Campbell, C., and Barkworth, M. (1987). Grass  
799 systematics and evolution (Washington DC: Random House (Smithsonian  
800 Institution Press)).

801 Covington, M.F., and Harmer, S.L. (2007). The circadian clock regulates auxin  
802 signaling and responses in *Arabidopsis*. *PLoS biology* 5, e222.

803 Dreni, L., and Kater, M.M. (2014). MADS reloaded: evolution of the AGAMOUS  
804 subfamily genes. *New Phytologist* 201, 717-732.

805 Druka, A., Franckowiak, J., Lundqvist, U., Bonar, N., Alexander, J., Houston, K.,  
806 Radovic, S., Shahinnia, F., Vendramin, V., Morgante, M., Stein, N., and Waugh,  
807 R. (2011). Genetic dissection of barley morphology and development. *Plant*  
808 *Physiol* 155, 617-627.

809 Forster, B.P., Franckowiak, J.D., Lundqvist, U., Lyon, J., Pitkethly, I., and Thomas,  
810 W.T. (2007). The barley phytomer. *Ann Bot* 100, 725-733.

811 Gaufichon, L., Marmagne, A., Belcram, K., Yoneyama, T., Sakakibara, Y., Hase, T.,  
812 Grandjean, O., Clément, G., Citerne, S., and Boutet-Mercey, S. (2017). ASN 1-  
813 encoded asparagine synthetase in floral organs contributes to nitrogen filling in  
814 *Arabidopsis* seeds. *The Plant Journal* 91, 371-393.

815 Gottwald, S., Bauer, P., Komatsuda, T., Lundqvist, U., and Stein, N. (2009). TILLING  
816 in the two-rowed barley cultivar 'Barke' reveals preferred sites of functional  
817 diversity in the gene HvHox1. *BMC Res Notes* 2, 258.

818 Hanzawa, Y., Money, T., and Bradley, D. (2005). A single amino acid converts a  
819 repressor to an activator of flowering. *Proc Natl Acad Sci U S A* 102, 7748-7753.

820 Hartmann, U., Höhmann, S., Nettesheim, K., Wisman, E., Saedler, H., and Huijser, P.  
821 (2000). Molecular cloning of SVP: a negative regulator of the floral transition in  
822 *Arabidopsis*. *The Plant Journal* 21, 351-360.

823 Hyun, Y., Richter, R., Vincent, C., Martinez-Gallegos, R., Porri, A., and Coupland, G.  
824 (2016). Multi-layered regulation of SPL15 and cooperation with SOC1 integrate  
825 endogenous flowering pathways at the *Arabidopsis* shoot meristem.  
826 *Developmental cell* 37, 254-266.

827 Jayakodi, M., Padmarasu, S., Haberer, G., Bonthala, V.S., Gundlach, H., Monat, C.,  
828 Lux, T., Kamal, N., Lang, D., Himmelbach, A., Ens, J., Zhang, X.-Q., Angessa,  
829 T.T., Zhou, G., Tan, C., Hill, C., Wang, P., Schreiber, M., Boston, L.B., Plott, C.,  
830 Jenkins, J., Guo, Y., Fiebig, A., Budak, H., Xu, D., Zhang, J., Wang, C.,  
831 Grimwood, J., Schmutz, J., Guo, G., Zhang, G., Mochida, K., Hirayama, T.,  
832 Sato, K., Chalmers, K.J., Langridge, P., Waugh, R., Pozniak, C.J., Scholz, U.,  
833 Mayer, K.F.X., Spannagl, M., Li, C., Mascher, M., and Stein, N. (2020). The  
834 barley pan-genome reveals the hidden legacy of mutation breeding. *Nature* 588,  
835 284-289.

836 Kellogg, E.A., Camara, P.E.A.S., Rudall, P.J., Ladd, P., Malcomber, S.T., Whipple,  
837 C.J., and Doust, A.N. (2013). Early inflorescence development in the grasses  
838 (Poaceae). *Frontiers in Plant Science* 4.

839 Kirby, E.M., and Appleyard, M. (1984). Cereal development guide. Cereal development  
840 guide. 2nd Edition.

841 Komatsuda, T., Pourkheirandish, M., He, C., Azhaguvel, P., Kanamori, H., Perovic, D.,  
842 Stein, N., Graner, A., Wicker, T., Tagiri, A., Lundqvist, U., Fujimura, T.,  
843 Matsuoka, M., Matsumoto, T., and Yano, M. (2007). Six-rowed barley originated  
844 from a mutation in a homeodomain-leucine zipper I-class homeobox gene.  
845 *Proceedings of the National Academy of Sciences* 104, 1424-1429.

846 Koppolu, R., and Schnurbusch, T. (2019). Developmental pathways for shaping spike  
847 inflorescence architecture in barley and wheat. *Journal of Integrative Plant  
848 Biology* 61, 278-295.

849 Koppolu, R., Anwar, N., Sakuma, S., Tagiri, A., Lundqvist, U., Pourkheirandish, M.,  
850 Rutten, T., Seiler, C., Himmelbach, A., Ariyadasa, R., Youssef, H.M., Stein, N.,  
851 Sreenivasulu, N., Komatsuda, T., and Schnurbusch, T. (2013). Six-rowed  
852 spike4 (Vrs4) controls spikelet determinacy and row-type in barley. *Proceedings  
853 of the National Academy of Sciences* 110, 13198-13203.

854 Lee, J.H., Yoo, S.J., Park, S.H., Hwang, I., Lee, J.S., and Ahn, J.H. (2007). Role of  
855 SVP in the control of flowering time by ambient temperature in *Arabidopsis*.  
856 *Genes & development* 21, 397-402.

857 Li, W., Wang, H., and Yu, D. (2016). *Arabidopsis* WRKY Transcription Factors  
858 WRKY12 and WRKY13 Oppositely Regulate Flowering under Short-Day  
859 Conditions. *Mol Plant* 9, 1492-1503.

860 Li, Y., Shen, Y., Cai, C., Zhong, C., Zhu, L., Yuan, M., and Ren, H. (2010). The type II  
861 *Arabidopsis* formin14 interacts with microtubules and microfilaments to regulate  
862 cell division. *The Plant Cell* 22, 2710-2726.

863 Lyu, J., Huang, L., Zhang, S., Zhang, Y., He, W., Zeng, P., Zeng, Y., Huang, G., Zhang,  
864 J., Ning, M., Bao, Y., Zhao, S., Fu, Q., Wade, L.J., Chen, H., Wang, W., and Hu,  
865 F. (2020). Neo-functionalization of a Teosinte branched 1 homologue mediates  
866 adaptations of upland rice. *Nat Commun* 11.

867 Michaels, S.D., Ditta, G., Gustafson-Brown, C., Pelaz, S., Yanofsky, M., and Amasino,  
868 R.M. (2003). AGL24 acts as a promoter of flowering in *Arabidopsis* and is  
869 positively regulated by vernalization. *The Plant Journal* 33, 867-874.

870 Ramsay, L., Comadran, J., Druka, A., Marshall, D.F., Thomas, W.T., Macaulay, M.,  
871 MacKenzie, K., Simpson, C., Fuller, J., Bonar, N., Hayes, P.M., Lundqvist, U.,  
872 Franckowiak, J.D., Close, T.J., Muehlbauer, G.J., and Waugh, R. (2011).  
873 INTERMEDIUM-C, a modifier of lateral spikelet fertility in barley, is an ortholog

874 of the maize domestication gene TEOSINTE BRANCHED 1. *Nat Genet* 43, 169-  
875 172.

876 Saisho, D., Pourkheirandish, M., Kanamori, H., Matsumoto, T., and Komatsuda, T.  
877 (2009). Allelic variation of row type gene *Vrs1* in barley and implication of the  
878 functional divergence. *Breeding Sci* 59, 621-628.

879 Sakuma, S., Salomon, B., and Komatsuda, T. (2011). The domestication syndrome  
880 genes responsible for the major changes in plant form in the Triticeae crops.  
881 *Plant Cell Physiol* 52, 738-749.

882 Sakuma, S., Pourkheirandish, M., Matsumoto, T., Koba, T., and Komatsuda, T. (2010).  
883 Duplication of a well-conserved homeodomain-leucine zipper transcription  
884 factor gene in barley generates a copy with more specific functions. *Funct Integr  
885 Genomics* 10, 123-133.

886 Sakuma, S., Pourkheirandish, M., Hensel, G., Kumlehn, J., Stein, N., Tagiri, A., Yamaji,  
887 N., Ma, J.F., Sassa, H., Koba, T., and Komatsuda, T. (2013). Divergence of  
888 expression pattern contributed to neofunctionalization of duplicated HD-Zip I  
889 transcription factor in barley. *New Phytol* 197, 939-948.

890 Sakuma, S., Lundqvist, U., Kakei, Y., Thirulogachandar, V., Suzuki, T., Hori, K., Wu,  
891 J., Tagiri, A., Rutten, T., Koppolu, R., Shimada, Y., Houston, K., Thomas,  
892 W.T.B., Waugh, R., Schnurbusch, T., and Komatsuda, T. (2017). Extreme  
893 Suppression of Lateral Floret Development by a Single Amino Acid Change in  
894 the VRS1 Transcription Factor. *Plant Physiol* 175, 1720-1731.

895 Sakuma, S., Golan, G., Guo, Z., Ogawa, T., Tagiri, A., Sugimoto, K., Bernhardt, N.,  
896 Brassac, J., Mascher, M., Hensel, G., Ohnishi, S., Jinno, H., Yamashita, Y.,  
897 Ayalon, I., Peleg, Z., Schnurbusch, T., and Komatsuda, T. (2019). Unleashing  
898 floret fertility in wheat through the mutation of a homeobox gene. *Proceedings  
899 of the National Academy of Sciences* 116, 5182-5187.

900 Sessa, G., Morelli, G., and Ruberti, I. (1993). The Athb-1 and-2 HD-Zip domains  
901 homodimerize forming complexes of different DNA binding specificities. *The  
902 EMBO journal* 12, 3507.

903 Shao, J., Haider, I., Xiong, L., Zhu, X., Hussain, R.M.F., Övernäs, E., Meijer, A.H.,  
904 Zhang, G., Wang, M., Bouwmeester, H.J., and Ouwerkerk, P.B.F. (2018).  
905 Functional analysis of the HD-Zip transcription factor genes *Oshox12* and  
906 *Oshox14* in rice. *PLOS ONE* 13, e0199248.

907 Thiel, J., Koppolu, R., Trautewig, C., Hertig, C., Kale, S.M., Erbe, S., Mascher, M.,  
908 Himmelbach, A., Rutten, T., Esteban, E., Pasha, A., Kumlehn, J., Provart, N.J.,  
909 Vanderauwera, S., Frohberg, C., and Schnurbusch, T. (2021). Transcriptional  
910 landscapes of floral meristems in barley. *Science Advances* 7, eabf0832.

911 Thirulogachandar, V., Alqudah, A.M., Koppolu, R., Rutten, T., Graner, A., Hensel, G.,  
912 Kumlehn, J., Brautigam, A., Sreenivasulu, N., Schnurbusch, T., and Kuhlmann,  
913 M. (2017). Leaf primordium size specifies leaf width and vein number among  
914 row-type classes in barley. *Plant J* 91, 601-612.

915 Tian, T., Liu, Y., Yan, H., You, Q., Yi, X., Du, Z., Xu, W., and Su, Z. (2017). agriGO v2.  
916 0: a GO analysis toolkit for the agricultural community, 2017 update. *Nucleic  
917 acids research* 45, W122-W129.

918 Tokunaga, H., Kojima, M., Kuroha, T., Ishida, T., Sugimoto, K., Kiba, T., and  
919 Sakakibara, H. (2012). *Arabidopsis lonely guy* (LOG) multiple mutants reveal a  
920 central role of the LOG-dependent pathway in cytokinin activation. *The Plant  
921 Journal* 69, 355-365.

922 Ullrich, S.E. (2011). Barley. Production, improvement, and uses. (Oxford: Wiley-  
923 Blackwell).

924 van Esse, G.W., Walla, A., Finke, A., Koornneef, M., Pecinka, A., and Von Korff, M.  
925 (2017). Six-rowed spike 3 (VRS3) is a histone demethylase that controls lateral  
926 spikelet development in barley. *Plant physiology*, pp. 00108.02017.  
927 Waddington, S.R., Cartwright, P.M., and Wall, P.C. (1983). A Quantitative Scale of  
928 Spike Initial and Pistil Development in Barley and Wheat. *Ann Bot-London* 51,  
929 119-130.  
930 Wang, Y., Yu, H., Tian, C., Sajjad, M., Gao, C., Tong, Y., Wang, X., and Jiao, Y. (2017).  
931 Transcriptome Association Identifies Regulators of Wheat Spike Architecture.  
932 *Plant Physiology* 175, 746-757.  
933 Wu, T.-Y., Krishnamoorthi, S., Goh, H., Leong, R., Sanson, A.C., and Urano, D. (2020).  
934 Crosstalk between heterotrimeric G protein-coupled signaling pathways and  
935 WRKY transcription factors modulating plant responses to suboptimal  
936 micronutrient conditions. *Journal of experimental botany* 71, 3227-3239.  
937 Youssef, H.M., Eggert, K., Koppolu, R., Alqudah, A.M., Poursarebani, N., Fazeli, A.,  
938 Sakuma, S., Tagiri, A., Rutten, T., and Govind, G. (2017). VRS2 regulates  
939 hormone-mediated inflorescence patterning in barley. *Nature Genetics* 49, 157-  
940 161.  
941 Yu, H., Xu, Y., Tan, E.L., and Kumar, P.P. (2002). AGAMOUS-LIKE 24, a dosage-  
942 dependent mediator of the flowering signals. *Proceedings of the National  
943 Academy of Sciences* 99, 16336-16341.  
944 Zhao, M., Yang, S., Chen, C.-Y., Li, C., Shan, W., Lu, W., Cui, Y., Liu, X., and Wu, K.  
945 (2015). Arabidopsis BREVIPEDICELLUS interacts with the SWI2/SNF2  
946 chromatin remodeling ATPase BRAHMA to regulate KNAT2 and KNAT6  
947 expression in control of inflorescence architecture. *PLoS genetics* 11,  
948 e1005125.  
949 Zwirek, M., Waugh, R., and McKim, S.M. (2019). Interaction between row-type genes  
950 in barley controls meristem determinacy and reveals novel routes to improved  
951 grain. *New Phytologist* 221, 1950-1965.  
952  
953

## Parsed Citations

Arce, A.L., Raineri, J., Capella, M., Cabello, J.V., and Chan, R.L. (2011). Uncharacterized conserved motifs outside the HD-Zip domain in HD-Zip subfamily I transcription factors; a potential source of functional diversity. *BMC Plant Biol* 11, 42.  
Google Scholar: [Author Only](#) [Title Only](#) [Author and Title](#)

Ariel, F.D., Manavella, P.A., Dezar, C.A., and Chan, R.L. (2007). The true story of the HD-Zip family. *Trends Plant Sci* 12, 419-426.  
Google Scholar: [Author Only](#) [Title Only](#) [Author and Title](#)

Bonnett, O.T. (1935). The development of the barley spike. *Journal of Agricultural Research* 51, 451-457.  
Google Scholar: [Author Only](#) [Title Only](#) [Author and Title](#)

Bull, H., Casao, M.C., Zwirek, M., Flavell, A.J., Thomas, W.T.B., Guo, W.B., Zhang, R.X., Rapazote-Flores, P., Kyriakidis, S., Russell, J., Druka, A., McKim, S.M., and Waugh, R. (2017). Barley SIX-ROWED SPIKE3 encodes a putative Jumonji C-type H3K9me2/me3 demethylase that represses lateral spikelet fertility. *Nat Commun* 8.  
Google Scholar: [Author Only](#) [Title Only](#) [Author and Title](#)

Capella, M., Re, D.A., Arce, A.L., and Chan, R.L. (2014). Plant homeodomain-leucine zipper I transcription factors exhibit different functional A/H motifs that selectively interact with TBP or/and TFIIB. *Plant Cell Rep* 33, 955-967.  
Google Scholar: [Author Only](#) [Title Only](#) [Author and Title](#)

Casas, A.M., Contreras-Moreira, B., Cantalapiedra, C.P., Sakuma, S., Gracia, M.P., Moralejo, M., Molina-Cano, J.L., Komatsuda, T., and Igartua, E. (2018). Resequencing the Vrs1 gene in Spanish barley landraces revealed reversion of six-rowed to two-rowed spike. *Molecular Breeding* 38, 51.  
Google Scholar: [Author Only](#) [Title Only](#) [Author and Title](#)

Chakraborty, N., Kanyuka, K., Jaiswal, D.K., Kumar, A., Arora, V., Malik, A., Gupta, N., Hooley, R., and Raghuram, N. (2019). GCR1 and GPA1 coupling regulates nitrate, cell wall, immunity and light responses in *Arabidopsis*. *Sci Rep-Uk* 9, 1-17.  
Google Scholar: [Author Only](#) [Title Only](#) [Author and Title](#)

Clifford, H., Soderstrom, T., Hilu, K., Campbell, C., and Barkworth, M. (1987). *Grass systematics and evolution* (Washington DC: Random House (Smithsonian Institution Press)).

Covington, M.F., and Harmer, S.L. (2007). The circadian clock regulates auxin signaling and responses in *Arabidopsis*. *PLoS biology* 5, e222.  
Google Scholar: [Author Only](#) [Title Only](#) [Author and Title](#)

Dreni, L., and Kater, M.M. (2014). MADS reloaded: evolution of the AGAMOUS subfamily genes. *New Phytologist* 201, 717-732.  
Google Scholar: [Author Only](#) [Title Only](#) [Author and Title](#)

Druka, A., Franckowiak, J., Lundqvist, U., Bonar, N., Alexander, J., Houston, K., Radovic, S., Shahinnia, F., Vendramin, V., Morgante, M., Stein, N., and Waugh, R. (2011). Genetic dissection of barley morphology and development. *Plant Physiol* 155, 617-627.  
Google Scholar: [Author Only](#) [Title Only](#) [Author and Title](#)

Forster, B.P., Franckowiak, J.D., Lundqvist, U., Lyon, J., Pitkethly, I., and Thomas, W.T. (2007). The barley phytomer. *Ann Bot* 100, 725-733.  
Google Scholar: [Author Only](#) [Title Only](#) [Author and Title](#)

Gaufichon, L., Marmagne, A., Belcram, K., Yoneyama, T., Sakakibara, Y., Hase, T., Grandjean, O., Clément, G., Citerne, S., and Boutet-Mercey, S. (2017). ASN 1-encoded asparagine synthetase in floral organs contributes to nitrogen filling in *Arabidopsis* seeds. *The Plant Journal* 91, 371-393.  
Google Scholar: [Author Only](#) [Title Only](#) [Author and Title](#)

Gottwald, S., Bauer, P., Komatsuda, T., Lundqvist, U., and Stein, N. (2009). TILLING in the two-rowed barley cultivar 'Barke' reveals preferred sites of functional diversity in the gene HvHox1. *BMC Res Notes* 2, 258.  
Google Scholar: [Author Only](#) [Title Only](#) [Author and Title](#)

Hanzawa, Y., Money, T., and Bradley, D. (2005). A single amino acid converts a repressor to an activator of flowering. *Proc Natl Acad Sci U S A* 102, 7748-7753.  
Google Scholar: [Author Only](#) [Title Only](#) [Author and Title](#)

Hartmann, U., Höhmann, S., Nettesheim, K., Wisman, E., Saedler, H., and Huijser, P. (2000). Molecular cloning of SVP: a negative regulator of the floral transition in *Arabidopsis*. *The Plant Journal* 21, 351-360.  
Google Scholar: [Author Only](#) [Title Only](#) [Author and Title](#)

Hyun, Y., Richter, R., Vincent, C., Martinez-Gallegos, R., Porri, A., and Coupland, G. (2016). Multi-layered regulation of SPL15 and cooperation with SOC1 integrate endogenous flowering pathways at the *Arabidopsis* shoot meristem. *Developmental cell* 37, 254-266.  
Google Scholar: [Author Only](#) [Title Only](#) [Author and Title](#)

Jayakodi, M., Padmarasu, S., Haberer, G., Bonthala, V.S., Gundlach, H., Monat, C., Lux, T., Kamal, N., Lang, D., Himmelbach, A., Ens, J., Zhang, X.-Q., Angessa, T.T., Zhou, G., Tan, C., Hill, C., Wang, P., Schreiber, M., Boston, L.B., Plott, C., Jenkins, J., Guo, Y., Fiebig, A., Budak, H., Xu, D., Zhang, J., Wang, C., Grimwood, J., Schmutz, J., Guo, G., Zhang, G., Mochida, K., Hirayama, T., Sato, K., Chalmers, K.J., Langridge, P., Waugh, R., Pozniak, C.J., Scholz, U., Mayer, K.F.X., Spannagl, M., Li, C., Mascher, M., and Stein, N. (2020). The barley

pan-genome reveals the hidden legacy of mutation breeding. *Nature* 588, 284-289.

Google Scholar: [Author Only](#) [Title Only](#) [Author and Title](#)

**Kellogg, E.A., Camara, P.E.A.S., Rudall, P.J., Ladd, P., Malcomber, S.T., Whipple, C.J., and Doust, A.N. (2013). Early inflorescence development in the grasses (Poaceae). *Frontiers in Plant Science* 4.**

Google Scholar: [Author Only](#) [Title Only](#) [Author and Title](#)

**Kirby, E.M., and Appleyard, M. (1984). Cereal development guide. Cereal development guide. 2nd Edition.**

Google Scholar: [Author Only](#) [Title Only](#) [Author and Title](#)

**Komatsuda, T., Pourkheirandish, M., He, C., Azhaguvvel, P., Kanamori, H., Perovic, D., Stein, N., Graner, A., Wicker, T., Tagiri, A., Lundqvist, U., Fujimura, T., Matsuoka, M., Matsumoto, T., and Yano, M. (2007). Six-rowed barley originated from a mutation in a homeodomain-leucine zipper I-class homeobox gene. *Proceedings of the National Academy of Sciences* 104, 1424-1429.**

Google Scholar: [Author Only](#) [Title Only](#) [Author and Title](#)

**Koppolu, R., and Schnurbusch, T. (2019). Developmental pathways for shaping spike inflorescence architecture in barley and wheat. *Journal of Integrative Plant Biology* 61, 278-295.**

Google Scholar: [Author Only](#) [Title Only](#) [Author and Title](#)

**Koppolu, R., Anwar, N., Sakuma, S., Tagiri, A., Lundqvist, U., Pourkheirandish, M., Rutten, T., Seiler, C., Himmelbach, A., Ariyadasa, R., Youssef, H.M., Stein, N., Sreenivasulu, N., Komatsuda, T., and Schnurbusch, T. (2013). Six-rowed spike4 (Vrs4) controls spikelet determinacy and row-type in barley. *Proceedings of the National Academy of Sciences* 110, 13198-13203.**

Google Scholar: [Author Only](#) [Title Only](#) [Author and Title](#)

**Lee, J.H., Yoo, S.J., Park, S.H., Hwang, I., Lee, J.S., and Ahn, J.H. (2007). Role of SVP in the control of flowering time by ambient temperature in *Arabidopsis*. *Genes & development* 21, 397-402.**

Google Scholar: [Author Only](#) [Title Only](#) [Author and Title](#)

**Li, W., Wang, H., and Yu, D. (2016). *Arabidopsis* WRKY Transcription Factors WRKY12 and WRKY13 Oppositely Regulate Flowering under Short-Day Conditions. *Mol Plant* 9, 1492-1503.**

Google Scholar: [Author Only](#) [Title Only](#) [Author and Title](#)

**Li, Y., Shen, Y., Cai, C., Zhong, C., Zhu, L., Yuan, M., and Ren, H. (2010). The type II *Arabidopsis* formin14 interacts with microtubules and microfilaments to regulate cell division. *The Plant Cell* 22, 2710-2726.**

Google Scholar: [Author Only](#) [Title Only](#) [Author and Title](#)

**Lyu, J., Huang, L., Zhang, S., Zhang, Y., He, W., Zeng, P., Zeng, Y., Huang, G., Zhang, J., Ning, M., Bao, Y., Zhao, S., Fu, Q., Wade, L.J., Chen, H., Wang, W., and Hu, F. (2020). Neo-functionalization of a Teosinte branched 1 homologue mediates adaptations of upland rice. *Nat Commun* 11.**

Google Scholar: [Author Only](#) [Title Only](#) [Author and Title](#)

**Michaels, S.D., Ditta, G., Gustafson-Brown, C., Pelaz, S., Yanofsky, M., and Amasino, R.M. (2003). AGL24 acts as a promoter of flowering in *Arabidopsis* and is positively regulated by vernalization. *The Plant Journal* 33, 867-874.**

Google Scholar: [Author Only](#) [Title Only](#) [Author and Title](#)

**Ramsay, L., Comadran, J., Druka, A., Marshall, D.F., Thomas, W.T., Macaulay, M., MacKenzie, K., Simpson, C., Fuller, J., Bonar, N., Hayes, P.M., Lundqvist, U., Franckowiak, J.D., Close, T.J., Muehlbauer, G.J., and Waugh, R. (2011). INTERMEDIUM-C, a modifier of lateral spikelet fertility in barley, is an ortholog of the maize domestication gene TEOSINTE BRANCHED 1. *Nat Genet* 43, 169-172.**

Google Scholar: [Author Only](#) [Title Only](#) [Author and Title](#)

**Saisho, D., Pourkheirandish, M., Kanamori, H., Matsumoto, T., and Komatsuda, T. (2009). Allelic variation of row type gene Vrs1 in barley and implication of the functional divergence. *Breeding Sci* 59, 621-628.**

Google Scholar: [Author Only](#) [Title Only](#) [Author and Title](#)

**Sakuma, S., Salomon, B., and Komatsuda, T. (2011). The domestication syndrome genes responsible for the major changes in plant form in the Triticeae crops. *Plant Cell Physiol* 52, 738-749.**

Google Scholar: [Author Only](#) [Title Only](#) [Author and Title](#)

**Sakuma, S., Pourkheirandish, M., Matsumoto, T., Koba, T., and Komatsuda, T. (2010). Duplication of a well-conserved homeodomain-leucine zipper transcription factor gene in barley generates a copy with more specific functions. *Funct Integr Genomics* 10, 123-133.**

Google Scholar: [Author Only](#) [Title Only](#) [Author and Title](#)

**Sakuma, S., Pourkheirandish, M., Hensel, G., Kumlehn, J., Stein, N., Tagiri, A., Yamaji, N., Ma, J.F., Sassa, H., Koba, T., and Komatsuda, T. (2013). Divergence of expression pattern contributed to neofunctionalization of duplicated HD-Zip I transcription factor in barley. *New Phytol* 197, 939-948.**

Google Scholar: [Author Only](#) [Title Only](#) [Author and Title](#)

**Sakuma, S., Lundqvist, U., Kakei, Y., Thirulogachandar, V., Suzuki, T., Hori, K., Wu, J., Tagiri, A., Rutten, T., Koppolu, R., Shimada, Y., Houston, K., Thomas, W.T.B., Waugh, R., Schnurbusch, T., and Komatsuda, T. (2017). Extreme Suppression of Lateral Floret Development by a Single Amino Acid Change in the VRS1 Transcription Factor. *Plant Physiol* 175, 1720-1731.**

Google Scholar: [Author Only](#) [Title Only](#) [Author and Title](#)

**Sakuma, S., Golan, G., Guo, Z., Ogawa, T., Tagiri, A., Sugimoto, K., Bernhardt, N., Brassac, J., Mascher, M., Hensel, G., Ohnishi, S.,**

Jinno, H., Yamashita, Y., Ayalon, I., Peleg, Z., Schnurbusch, T., and Komatsuda, T. (2019). Unleashing floret fertility in wheat through the mutation of a homeobox gene. *Proceedings of the National Academy of Sciences* 116, 5182-5187.

Google Scholar: [Author Only](#) [Title Only](#) [Author and Title](#)

Sessa, G., Morelli, G., and Ruberti, I. (1993). The Athb-1 and-2 HD-Zip domains homodimerize forming complexes of different DNA binding specificities. *The EMBO journal* 12, 3507.

Google Scholar: [Author Only](#) [Title Only](#) [Author and Title](#)

Shao, J., Haider, I., Xiong, L., Zhu, X., Hussain, R.M.F., Övernäs, E., Meijer, A.H., Zhang, G., Wang, M., Bouwmeester, H.J., and Ouwerkerk, P.B.F. (2018). Functional analysis of the HD-Zip transcription factor genes Oshox12 and Oshox14 in rice. *PLOS ONE* 13, e0199248.

Google Scholar: [Author Only](#) [Title Only](#) [Author and Title](#)

Thiel, J., Koppolu, R., Trautewig, C., Hertig, C., Kale, S.M., Erbe, S., Mascher, M., Himmelbach, A., Rutten, T., Esteban, E., Pasha, A., Kumlein, J., Provart, N.J., Vanderauwera, S., Frohberg, C., and Schnurbusch, T. (2021). Transcriptional landscapes of floral meristems in barley. *Science Advances* 7, eabf0832.

Google Scholar: [Author Only](#) [Title Only](#) [Author and Title](#)

Thirulogachandar, V., Alqudah, A.M., Koppolu, R., Rutten, T., Graner, A., Hensel, G., Kumlein, J., Brautigam, A., Sreenivasulu, N., Schnurbusch, T., and Kuhlmann, M. (2017). Leaf primordium size specifies leaf width and vein number among row-type classes in barley. *Plant J* 91, 601-612.

Google Scholar: [Author Only](#) [Title Only](#) [Author and Title](#)

Tian, T., Liu, Y., Yan, H., You, Q., Yi, X., Du, Z., Xu, W., and Su, Z. (2017). agriGO v2. 0: a GO analysis toolkit for the agricultural community, 2017 update. *Nucleic acids research* 45, W122-W129.

Google Scholar: [Author Only](#) [Title Only](#) [Author and Title](#)

Tokunaga, H., Kojima, M., Kuroha, T., Ishida, T., Sugimoto, K., Kiba, T., and Sakakibara, H. (2012). *Arabidopsis lonely guy* (LOG) multiple mutants reveal a central role of the LOG-dependent pathway in cytokinin activation. *The Plant Journal* 69, 355-365.

Google Scholar: [Author Only](#) [Title Only](#) [Author and Title](#)

Ullrich, S.E. (2011). Barley. Production, improvement, and uses. (Oxford: Wiley-Blackwell).

Google Scholar: [Author Only](#) [Title Only](#) [Author and Title](#)

van Esse, G.W., Walla, A., Finke, A., Koornneef, M., Pecinka, A., and Von Korff, M. (2017). Six-rowed spike 3 (VRS3) is a histone demethylase that controls lateral spikelet development in barley. *Plant physiology*, pp. 00108.02017.

Google Scholar: [Author Only](#) [Title Only](#) [Author and Title](#)

Waddington, S.R., Cartwright, P.M., and Wall, P.C. (1983). A Quantitative Scale of Spike Initial and Pistil Development in Barley and Wheat. *Ann Bot-London* 51, 119-130.

Google Scholar: [Author Only](#) [Title Only](#) [Author and Title](#)

Wang, Y., Yu, H., Tian, C., Sajjad, M., Gao, C., Tong, Y., Wang, X., and Jiao, Y. (2017). Transcriptome Association Identifies Regulators of Wheat Spike Architecture. *Plant Physiology* 175, 746-757.

Google Scholar: [Author Only](#) [Title Only](#) [Author and Title](#)

Wu, T.-Y., Krishnamoorthi, S., Goh, H., Leong, R., Sanson, A.C., and Urano, D. (2020). Crosstalk between heterotrimeric G protein-coupled signaling pathways and WRKY transcription factors modulating plant responses to suboptimal micronutrient conditions. *Journal of experimental botany* 71, 3227-3239.

Google Scholar: [Author Only](#) [Title Only](#) [Author and Title](#)

Youssef, H.M., Eggert, K., Koppolu, R., Alqudah, A.M., Poursarebani, N., Fazeli, A., Sakuma, S., Tagiri, A., Rutten, T., and Govind, G. (2017). VRS2 regulates hormone-mediated inflorescence patterning in barley. *Nature Genetics* 49, 157-161.

Google Scholar: [Author Only](#) [Title Only](#) [Author and Title](#)

Yu, H., Xu, Y., Tan, E.L., and Kumar, P.P. (2002). AGAMOUS-LIKE 24, a dosage-dependent mediator of the flowering signals. *Proceedings of the National Academy of Sciences* 99, 16336-16341.

Google Scholar: [Author Only](#) [Title Only](#) [Author and Title](#)

Zhao, M., Yang, S., Chen, C.-Y., Li, C., Shan, W., Lu, W., Cui, Y., Liu, X., and Wu, K. (2015). *Arabidopsis BREVPEDICELLUS* interacts with the SWI2/SNF2 chromatin remodeling ATPase BRAHMA to regulate KNAT2 and KNAT6 expression in control of inflorescence architecture. *PLoS genetics* 11, e1005125.

Google Scholar: [Author Only](#) [Title Only](#) [Author and Title](#)

Zwirek, M., Waugh, R., and McKim, S.M. (2019). Interaction between row-type genes in barley controls meristem determinacy and reveals novel routes to improved grain. *New Phytologist* 221, 1950-1965.

Google Scholar: [Author Only](#) [Title Only](#) [Author and Title](#)